International Journal of Engineering Science 125 (2018) 1–22

Contents lists available at ScienceDirect

International Journal of Engineering Science

journal homepage: www.elsevier.com/locate/ijengsci

Nonlocal nonlinear analysis of functionally graded plates using third-order shear deformation theory

S. Srividhya[a], P. Raghu[a], A. Rajagopal[a], J.N. Reddy[b,*]

[a] Department of Civil Engineering, Indian Institute of Technology Hyderabad, Kandi, Sangareddy, Telangana, India
[b] Department of Mechanical Engineering, Texas A&M University, College Station, Texas, USA

ARTICLE INFO

Article history:
Received 18 October 2017
Revised 1 December 2017
Accepted 8 December 2017

Keywords:
Functionally graded materials
Third-order plate theory
Eringen's stress-gradient model
The von Kármán nonlinearity
Nonlocal effects

ABSTRACT

In this work, nonlocal nonlinear analysis of functionally graded plates subjected to static loads is studied. The nonlocal nonlinear formulation is developed based on the third-order shear deformation theory (TSDT) of Reddy (1984, 2004). The von Kármán nonlinear strains are used and the governing equations of the TSDT are derived accounting for Eringen's nonlocal stress-gradient model (Eringen, 1998). The nonlinear displacement finite element model of the resulting governing equations is developed, and Newton's iterative procedure is used for the solution of nonlinear algebraic equations. The mechanical properties of functionally graded plate are assumed to vary continuously through the thickness and obey a power-law distribution of the volume fraction of the constituents. The variation of the volume fractions through the thickness have been computed using two different homogenization techniques, namely, the rule of mixtures and the Mori–Tanaka scheme. A detailed parametric study to show the effect of side-to-thickness ratio, power-law index, and nonlocal parameter on the load-deflection characteristics of plates have been presented. The stress results are compared with the first-order shear deformation theory (FSDT) to show the accuracy of nonlocal nonlinear TSDT formulation.

1. Introduction

Functionally graded materials (FGMs) are the special class of composites, in which the volume fraction of two or more materials are varied continuously as a function of position along certain dimension(s) of the structure to achieve a required functionality. The concept of FGMs was proposed by materials scientists, based on its use in applications such as thermal barrier materials (Koizumi, 1993; 1997). FGMs have many other applications such as Bio materials (Pompe et al., 2003), Dental implants (Watari, Yokoyama, Saso, & Kawasaki, 1997), Sensors, Thermo-generators (Aller, Drar, Schilz, & Kaysser, 2003) and wear resistant coatings (Schulz, Peters, Bach, & Tegeder, 2003). Due to smooth and continuous variation of material properties from one surface to the other, FGMs are usually superior to the conventional composite materials. FGMs possess a number of advantages, including a reduction of in-plane and transverse through-the-thickness stresses, an improved residual stress distribution, enhanced thermal properties, higher fracture toughness, and reduced stress intensity factors along with high wear resistance. Therefore, accurate determination of the deformation and stress variation in such structures is important. FGMs are mostly used in nano/micro components, in which it is necessary to account for small scale

* Corresponding author.
E-mail address: jnreddy@tamu.edu (J.N. Reddy).

https://doi.org/10.1016/j.ijengsci.2017.12.006
0020-7225/

effects, higher-order kinematics, and geometric nonlinearity. In view of this, the present work accounts for non locality, nonlinearity and higher-order kinematics through the TSDT (Reddy, 1984; 2004).

Micro structural and size effects play a dominant role when the structures such as nano beams made up of FGMs are used for structural purposes (Rahmani & Pedram, 2014; Simsek & Yurtcu, 2013). It has been observed that, the boundary value problems solved using a classical continuum mechanics approach cease to give solutions that are comparable to experimental solutions in case of micro/nano structures. The main reason for this discrepancy is that the classical continuum approach lacks an internal length scale that takes care of material micro structure. Many researchers have discussed the importance of size effects in nano/micro structures (John, George, & Richard, 2003; Kröner, 1967; Krumhansl, 1968; Kunin, 1984). Nonlocal continuum models are found to be superior to their local counterparts for the analysis of nano structures (Arash & Wang, 2012; Edelen & Laws, 1971). Many works discussed the importance of nonlocal theories in the analysis of beams and plates (Reddy, 2007a; 2010; Roque, Ferreira, & Reddy, 2011; Thai, 2012). The effect of non locality appears in the constitutive relations via a length scale parameter. These constitutive relations are also proven to avoid the singularity at the crack tip in Fracture mechanics (Zhou, Han, & Du, 1999). These models are also reported to achieve properly convergent solutions for localized damage analysis (Bažant & Milan, 2002). In the last two decades, Eringen's nonlocal theory (Eringen, 1972; 1983; Eringen & Edelen, 1972) has received significant attention. Eringen's stress gradient model is based on the assumption that the stress at a point is a function of the strain field at all neighboring points on the continuum. The interatomic forces and atomic length scales directly come in the constitutive equations as material parameters (Eringen, 2002). Recently, Eringen's model has been modified using the gradient elastic model as well as an integral non-local elastic model that is based on combining the local and the non-local curvatures in the constitutive elastic relations (Challamel & Wang, 2008; Fernández-Sáez, Zaeraa, Loyaa, & Reddy, 2016; Romano, Barretta, Diaco, & de Sciarra, 2017).

Modeling of material through the thickness for FGMs has been important for accurate analysis of FGMs. Some works on the variation of material properties through the thickness according to a power-law distribution and the locally effective material properties in terms of the volume fractions of the constituents through the Mori–Tanaka scheme includes Reddy and Cheng (2001) and Vel and Batra (2002). Kashtalyan (2004) derived the three-dimensional elasticity solution for a functionally graded simply supported plate subjected to transverse loading. A three-dimensional solution for the problem of clamped rectangular plates of arbitrary thickness is presented by Elishakoff and Gentilini (2005). Aghababaei and Reddy (2009) provided analytical solutions of bending and free vibration of plates using the nonlocal TSDT. Jandaghian and Rahmani (2016) provided analytical solutions of vibration analysis of functionally graded piezoelectric nano plates based on Eringen's non local theory and Kirchhoff plate theory. Analytical and finite element models of functionally graded plates using first order theory and third-order theory was presented by Reddy (2000). Many researchers have recently attempted to study the behavior of FGM plates using higher order theories (Aliaga & Reddy, 2004; Golmakani & Kadkhodayan, 2011; Reddy & Kim, 2012; Talha & Singh, 2010). Reddy (2010) presented the formulation for FGM plates considering a general third-order theory and the von Kármán nonlinear strains. Kim and Reddy (2015) presented the theory and finite element analysis of functionally graded plates with modified couple stress effect and the von Kármán nonlinearity. Mousavi, Paavola, and Reddy (2015) presented a variational approach based on Hamilton principle and developed the governing equations for the dynamic analysis of plates using the Reddy third-order shear deformable plate theory accounting for the strain gradient and velocity gradient effects. Ferreira, Batra, Rouque, Qian, and Martins (2005) and Qian, Batra, and Chen (2004) carried out analysis of FGM plates using higher order theories and meshless methods. Transient, thermo-elastic, bending and vibration analysis of the functionally graded plates using FSDT were presented by many researchers such as Praveen and Reddy (1998), Singha, Prakash, and Ganapathi (2011), Hosseini-Hashemi, Taher, Akhavan, and Omidi (2010), Reddy and Chin (1998). Reddy, El-Borgi, and Romanoff (2014) performed the nonlinear analysis of functionally graded micro beams using Eringen's nonlocal differential model. Rahaeifard, Kahrobaiyan, Ahmadian, and Firoozbakhsh (2013) applied strain gradient formulation to investigate the effect of length scale on the static and dynamic behavior of Euler–Bernoulli beams made of functionally graded materials. Salehipour, Shahidi, and Nahvi (2015) formulated a novel nonlocal theory that assumes the nonlocal strain at a point as a function of local strain at all neighboring points. This novel theory was applied to study the functionally graded plates using the first order plate theory and the results are validated with Eringen's three dimensional nonlocal models. Nejad and Hadi (2016) investigated bi-directional functionally graded Euler–Bernoulli nano beams subjected bending using Eringen's non-local elasticity theory. Recently Ghayesh, Farokhi, Gholipour, and Tavallaeinejad (2017) investigated the effect of the small scale parameter, the gradient index on the nonlinear behavior of functionally graded tapered beams subjected to bending and forced vibration. Here they used a modified couple stress theory to account for the size dependent behavior of the functionally graded material. Raghu, Rajagopal, and Reddy (2018) developed nonlinear finite element model using Eringen's nonlocal model and von Kármán nonlinear strains to analyze the laminated composite plates using Reddy's third-order shear deformation theory (Reddy, 1984).

In this paper, the formulation for nonlocal nonlinear analysis of FGM plates is presented. The behavior of FGM plates subjected to static loads is studied. The Reddy TSDT with the von Kármán nonlinear strains is used for deriving the governing equations that accounts for Eringen's nonlocal stress-gradient model. The nonlinear displacement finite element model is developed from the resulting nonlocal nonlinear equations. Two homogenization techniques, namely rule of mixtures and Mori–Tanaka scheme is used to find the mechanical properties of the FGM plate using power-law distribution of the volume fraction of the constituents. The presented results are compared with the literature and the percentage difference between the deflections obtained using two techniques are tabulated in the results. The effect of side-to-thickness ratio, power-law

index, and nonlocal parameter on the load-deflection characteristics of the plates has been presented. The effect of nonlocal parameter and the power-law index on axial and shear stress has also been presented.

Following this introduction, the nonlocal elasticity theory is discussed in Section 2. In Section 3 the mathematical idealization of FGM plate with the rule of mixtures and Mori–Tanaka scheme employing power-law distribution is explained. The governing equations are derived using TSDT in Section 4 and a finite element model is presented in Section 5. The numerical examples with the results and discussion is detailed in Section 6. Some conclusions are presented in Section 7.

2. Nonlocal elasticity theory

Most of the materials are heterogeneous at smaller length scales such as nano scale (Eringen, 1998). The classical continuum theories idealize the material as continuously distributed at macro scale there by abandoning the discreteness and heterogeneity of the material. This idealization can accurately predict the behavior of material at large scale, but this assumption in micro/nano electro mechanical systems cannot predict the accurate results. This is mainly due to the fact that the classical continuum approach lacks the material length scale parameter in the constitutive relations (Eringen & Edelen, 1972). In small scale structures the internal characteristic lengths such as the grain size and distance between the atoms is comparable to the spatial dimensions of the structure and hence the size effects are predominant (Eringen, 2002).

The nonlocal continuum mechanics was initiated by Eringen (1998) who proposed a constitutive model that expresses the nonlocal stress tensor $\boldsymbol{\sigma}^{nl}$ at point $\boldsymbol{x}$ as

$$\boldsymbol{\sigma}^{nl}(\boldsymbol{x}) = \int K(|\boldsymbol{x}' - \boldsymbol{x}|, \tau)\boldsymbol{\sigma}(\boldsymbol{x}')\, dv' \tag{1}$$

where $\boldsymbol{\sigma}(\boldsymbol{x}')$ is the classical macroscopic stress tensor at point $\boldsymbol{x}'$ and $K(|\boldsymbol{x}' - \boldsymbol{x}|, \tau)$ is the Kernel function which is normalized over the volume of the body represents the nonlocal modulus and τ is the material constant that depends on the internal characteristic length (e.g. lattice parameter, granular distance) and external characteristic length (e.g. crack length). From Eq. (1) it can be seen that the K has the units of (length)$^{-3}$. The Kernel function has the following properties (Eringen, 1983):

- The function attains it's maximum at $\boldsymbol{x} = \boldsymbol{x}'$ and attenuates with $|\boldsymbol{x}' - \boldsymbol{x}|$
- When $\tau \to 0$, K becomes Derac delta function. This makes nonlocal elasticity breaks down to classical elasticity.
- Kernel function K can be determined by matching the dispersion curves of plane waves with those of atomic lattice dynamics. For two dimensional case, it is found to be

$$K(|\boldsymbol{x}|, \tau) = (\pi \tau l^2)^{-1} exp(-\boldsymbol{x}.\boldsymbol{x}/l^2\tau) \tag{2}$$

Furthermore, K is assumed to be a Green's function of a linear differential operator $\mathcal{L}$:

$$\mathcal{L}K(|\boldsymbol{x}' - \boldsymbol{x}|, \tau) = \delta(|\boldsymbol{x}' - \boldsymbol{x}|) \tag{3}$$

Applying Eq. (3) to Eq. (1), we obtain

$$\mathcal{L}\sigma_{ij}^{nl} = \sigma_{ij} \tag{4}$$

If $\mathcal{L}$ is differential operator with constant coefficients, then it follows

$$(\mathcal{L}\sigma_{ij}^{nl})_{,k} = \mathcal{L}\sigma_{ij,k}^{nl} \tag{5}$$

Using the Eq. (5), the equilibrium equations of two dimensional linear elastic isotropic body can be expressed as

$$\sigma_{kl,k} + \mathcal{L}(\rho f_l - \rho \ddot{u}_l) = 0 \tag{6}$$

which is a partial differential equation to be solved instead of a integro-partial differential equation.

Eq. (4) can be represented equivalently in differential form as

$$\left(1 - \tau^2 l^2 \nabla^2\right)\boldsymbol{\sigma}^{nl} = \boldsymbol{\sigma} \tag{7}$$

where $\tau^2 = \frac{(e_0 a)^2}{l^2}$, e_0 is a material constant and a and l are the internal and external characteristic lengths, respectively. In general, ∇^2 is the three-dimensional Laplace operator. The nonlocal parameter μ can be taken as $\mu = \tau^2 l^2 = (e_0 a)^2$. In rectangular Cartesian component form, the relation can be written as (invoking Hooke's law for the local stress tensor components),

$$\mathcal{L}(\sigma_{ij}^{nl}) = \sigma_{ij} = C_{ijmn}\varepsilon_{mn} \tag{8}$$

3. Mathematical idealization of the FGM plate

Although FGMs are highly heterogeneous, it will be very useful to idealize them as continua with their mechanical properties changing smoothly with respect to the spatial coordinates. The homogenization schemes are necessary to simplify their complicated heterogeneous micro structures in order to analyze FGMs in an efficient manner. It is worth noting that, the distribution of material property in FGM structures may be designed to various spatial specifications. A typical FGM represents a particulate composite with a prescribed distribution of volume fractions of constituent phases. The material

properties are generally assumed to follow gradation through the thickness in a continuous manner. The effective properties of macroscopic homogeneous materials can be derived from the microscopic heterogeneous material structures using homogenization techniques (Birman & Byrd, 2007; Klusemann & Svendsen, 2010; Zuiker, 1995). Several models like the rule of mixtures (Praveen & Reddy, 1998; Reddy, 2000), Hashin–Shtrikman type bounds (Hashin & Shtrikman, 1962), Mori–Tanaka scheme (Mori & Tanaka, 1973; Zuiker, 1995) and Self consistent schemes (Willis, 1977) are available in the literature for determination of the bounds for the effective properties. Voigt scheme and the Mori–Tanaka scheme have been generally used for the study of FGM plates and structures by researchers (Ferreira et al., 2005; Shen & Wang, 2012) and have been adopted here.

3.1. Mori–Tanaka scheme

For those parts of the graded microstructure that have a well-defined continuous matrix and discontinuous reinforcement, the overall properties and local fields can be closely predicted by Mori–Tanaka estimates. The assumption of spherical particles embedded in a matrix is considered. The primary matrix phase is assumed to be reinforced by spherical particles of secondary phase. Zuiker (1995), Mori and Tanaka (1973) derived a method to calculate the average internal stress in the matrix of a material. This has been reformulated by Benveniste (1987) for use in the computation of the effective properties of composite materials. According to the Mori–Tanaka scheme, the effective elastic properties of the FGM can be expressed as

$$\frac{K-K_c}{K_m-K_c}=\frac{V_m}{1+(1-V_m)\dfrac{K_m-K_c}{K_c+\dfrac{4}{3}G_c}}$$
$$\frac{G-G_c}{G_m-G_c}=\frac{V_m}{1+(1-V_m)\dfrac{(G_m-G_c)}{G_c+f_c}} \tag{9}$$

where

$$f_c=\frac{G_c(9K_c+8G_c)}{6(K_c+2G_c)} \tag{10}$$

in which K and G are bulk modulus and shear modulus, respectively. The subscript c and m refer to ceramic and metal phases, respectively. K and G are related to Young's modulus and Poisson's ratio ν, by the following equations

$$E=\frac{9KG}{3K+G},\quad \nu=\frac{3K-2G}{2(3K+G)} \tag{11}$$

3.2. Voigt scheme – rule of mixture

With a certain mixture of ceramic and metal phases, the response of the composite is dependent upon factors such as the concentration, shape and contiguity, and spatial distribution of each phase. There are two extreme rule of mixture models to describe the effective mechanical properties of a composite comprising two elastically isotropic constituent phase: the Voigt and Reuss models (Hill, 1952). The Voigt model corresponds to the case when the applied load causes equal strains in the two phases. The overall composite stress is the sum of stresses carried by each phase.

Voigt scheme has been adopted in most analysis of FGM structures (Ferreira et al., 2005; Hosseini-Hashemi et al., 2010; Matsunaga, 2009; Reddy, 2000; Reddy & Cheng, 2001; Reddy & Chin, 1998; Singha et al., 2011; Vel & Batra, 2002; Talha & Singh, 2010). The advantage of the above model is the simplicity of implementation and the ease of computation. According to Voigt scheme, the effective properties are the arithmetic average of constituent properties and are given by Eq. (12).

$$E(z)=E_mV_m+E_cV_c \tag{12}$$

where, E_m and E_c represent the Young's modulus of metal and ceramic, respectively, V_m and V_c represent the volume fraction of metal and ceramic phase, respectively, which vary with respect to thickness coordinate z according to power law given in Eq. (13).

3.3. Power law for FGM plates

The variation of properties through the thickness is considered to be either exponential (called E-FGM) or based on a power series (called P-FGM) in the literature, which covers most of the existing analytical models. The Power law is most popular because of its simplicity and algebraic nature which is easy to implement.

The volume fraction of ceramic at any distance from the mid plane ($z=0$) can be expressed in the form of power law as

$$V_c=\left(\frac{1}{2}+\frac{z}{h}\right)^n \tag{13}$$

The sum of the volume fractions of all the constituent materials is unity. For a two constituent FGM plate (i.e. ceramic and metal), the volume fraction of metal can be written as

$$V_m = 1 - V_c \tag{14}$$

4. Theoretical formulation

4.1. Introduction

The classical plate theory and FSDT are the simplest equivalent single layer theories. The TSDT represents the kinematics more realistically and does not require shear correction factor that the FSDT requires. The TSDT of Reddy (1984) is based on a displacement field that includes the cubic term in the thickness coordinate (z), hence the transverse shear strain and hence stress are represented as quadratic through the plate thickness and also satisfies the stress free conditions on the bounding planes (top and bottom surfaces) of the plate. In spite of relatively more complex algebraic equations and computational effort compared to the classical and FSDT theories, the TSDT yields results that are close to 3-D elasticity solutions (Reddy & Wang, 1998; Reddy, 2007b). There are some articles that incorporate the third-order plate theory to obtain more accurate results (Lee & Reddy, 2004; Reddy, 1984; Reddy & Wang, 1998). Therefore, it is useful to study the extension of the third-order plate theory to include the length scale effects of Eringen's model.

4.2. Displacement fields and strains

The TSDT of Reddy (1984, 2004) is based on the displacement field

$$\begin{aligned} u_1(x,y,z) &= u(x,y) + z\phi_x - \frac{4z^3}{3h^2}\left(\phi_x + \frac{\partial w}{\partial x}\right) \\ u_2(x,y,z) &= v(x,y) + z\phi_y - \frac{4z^3}{3h^2}\left(\phi_y + \frac{\partial w}{\partial y}\right) \\ u_3(x,y,z) &= w(x,y) \end{aligned} \tag{15}$$

where (u_1, u_2, u_3) are the total displacements in the (x, y, z) coordinates and (u, v, w) are displacements of a point on the mid plane.

4.3. Strain–displacement relations

Substitution of displacements into the von Kármán non-linear strain displacement relation yields the strains as

$$\begin{Bmatrix} \varepsilon_{xx} \\ \varepsilon_{yy} \\ \gamma_{xy} \end{Bmatrix} = \begin{Bmatrix} \varepsilon_{xx}^{(0)} \\ \varepsilon_{yy}^{(0)} \\ \gamma_{xy}^{(0)} \end{Bmatrix} + z\begin{Bmatrix} \varepsilon_{xx}^{(1)} \\ \varepsilon_{yy}^{(1)} \\ \gamma_{xy}^{(1)} \end{Bmatrix} + z^3\begin{Bmatrix} \varepsilon_{xx}^{(3)} \\ \varepsilon_{yy}^{(3)} \\ \gamma_{xy}^{(3)} \end{Bmatrix} \tag{16}$$

$$\begin{Bmatrix} \gamma_{yz} \\ \gamma_{xz} \end{Bmatrix} = \begin{Bmatrix} \gamma_{yz}^{(0)} \\ \gamma_{xz}^{(0)} \end{Bmatrix} + z^2\begin{Bmatrix} \gamma_{yz}^{(2)} \\ \gamma_{xz}^{(2)} \end{Bmatrix} \tag{17}$$

where

$$\begin{Bmatrix} \varepsilon_{xx}^{(0)} \\ \varepsilon_{yy}^{(0)} \\ \gamma_{xy}^{(0)} \end{Bmatrix} = \begin{Bmatrix} \dfrac{\partial u}{\partial x} + \dfrac{1}{2}\left(\dfrac{\partial w}{\partial x}\right)^2 \\ \dfrac{\partial v}{\partial y} + \dfrac{1}{2}\left(\dfrac{\partial w}{\partial y}\right)^2 \\ \dfrac{\partial u}{\partial y} + \dfrac{\partial v}{\partial x} + \dfrac{\partial w}{\partial x}\dfrac{\partial w}{\partial y} \end{Bmatrix}, \quad \begin{Bmatrix} \varepsilon_{xx}^{(1)} \\ \varepsilon_{yy}^{(1)} \\ \gamma_{xy}^{(1)} \end{Bmatrix} = \begin{Bmatrix} \dfrac{\partial \phi_x}{\partial x} \\ \dfrac{\partial \phi_y}{\partial y} \\ \dfrac{\partial \phi_x}{\partial y} + \dfrac{\partial \phi_y}{\partial x} \end{Bmatrix} \tag{18}$$

$$\begin{Bmatrix} \varepsilon_{xx}^{(3)} \\ \varepsilon_{yy}^{(3)} \\ \gamma_{xy}^{(3)} \end{Bmatrix} = -c_1\begin{Bmatrix} \dfrac{\partial \phi_x}{\partial x} + \dfrac{\partial^2 w}{\partial x^2} \\ \dfrac{\partial \phi_y}{\partial y} + \dfrac{\partial^2 w}{\partial y^2} \\ \dfrac{\partial \phi_x}{\partial y} + \dfrac{\partial \phi_y}{\partial x} + 2\dfrac{\partial^2 w}{\partial x \partial y} \end{Bmatrix} \tag{19}$$

$$\begin{Bmatrix}\gamma_{yz}^{(0)}\\ \gamma_{xz}^{(0)}\end{Bmatrix}=\begin{Bmatrix}\phi_y+\dfrac{\partial w}{\partial y}\\ \phi_x+\dfrac{\partial w}{\partial x}\end{Bmatrix},\quad \begin{Bmatrix}\gamma_{yz}^{(2)}\\ \gamma_{xz}^{(2)}\end{Bmatrix}=-c_2\begin{Bmatrix}\phi_y+\dfrac{\partial w}{\partial y}\\ \phi_x+\dfrac{\partial w}{\partial x}\end{Bmatrix} \tag{20}$$

and

$$c_2=3c_1,\quad c_1=\frac{4}{3h^2} \tag{21}$$

4.4. Governing equilibrium equations

The following nonlocal nonlinear governing equations in terms of local stress resultants can be obtained by applying the operator $\mathcal{L}$ on both sides of the governing equations and by using the relation between local and nonlocal stress resultants given in Appendix A.

$$\frac{\partial N_{xx}}{\partial x}+\frac{\partial N_{xy}}{\partial y}=0 \tag{22}$$

$$\frac{\partial N_{xy}}{\partial x}+\frac{\partial N_{yy}}{\partial y}=0 \tag{23}$$

$$\frac{\partial \bar{Q}_x}{\partial x}+\frac{\partial \bar{Q}_y}{\partial y}+\frac{\partial}{\partial x}\left(N_{xx}\frac{\partial w}{\partial x}+N_{xy}\frac{\partial w}{\partial y}\right)+\frac{\partial}{\partial y}\left(N_{xy}\frac{\partial w}{\partial x}+N_{yy}\frac{\partial w}{\partial y}\right)$$
$$+c_1\left(\frac{\partial^2 P_{xx}}{\partial x^2}+2\frac{\partial^2 P_{xy}}{\partial x\partial y}+\frac{\partial^2 P_{yy}}{\partial y^2}\right)=-q(1-\mu\nabla^2) \tag{24}$$

$$\frac{\partial \bar{M}_{xx}}{\partial x}+\frac{\partial \bar{M}_{xy}}{\partial y}-\bar{Q}_x=0 \tag{25}$$

$$\frac{\partial \bar{M}_{xy}}{\partial x}+\frac{\partial \bar{M}_{yy}}{\partial y}-\bar{Q}_y=0 \tag{26}$$

where

$$\begin{Bmatrix}N_{\alpha\beta}\\ M_{\alpha\beta}\\ P_{\alpha\beta}\end{Bmatrix}=\int_{-\frac{h}{2}}^{\frac{h}{2}}\sigma_{\alpha\beta}\begin{Bmatrix}1\\ z\\ z^3\end{Bmatrix}dz,\quad \begin{Bmatrix}Q_\alpha\\ R_\alpha\end{Bmatrix}=\int_{-\frac{h}{2}}^{\frac{h}{2}}\sigma_{\alpha z}\begin{Bmatrix}1\\ z^2\end{Bmatrix}dz$$

and

$$\bar{M}_{\alpha\beta}=M_{\alpha\beta}-c_1P_{\alpha\beta},\quad \bar{Q}_\alpha=Q_\alpha-c_2R_\alpha \tag{27}$$

which are further simplified as

$$\begin{Bmatrix}\{N\}\\ \{M\}\\ \{P\}\end{Bmatrix}=\begin{bmatrix}[A] & [B] & [E]\\ [B] & [D] & [F]\\ [E] & [F] & [H]\end{bmatrix}\begin{Bmatrix}\{\varepsilon^{(0)}\}\\ \{\varepsilon^{(1)}\}\\ \{\varepsilon^{(3)}\}\end{Bmatrix} \tag{28}$$

$$\begin{Bmatrix}\{Q\}\\ \{R\}\end{Bmatrix}=\begin{bmatrix}[A] & [D]\\ [D] & [F]\end{bmatrix}\begin{Bmatrix}\{\gamma^{(0)}\}\\ \{\gamma^{(2)}\}\end{Bmatrix} \tag{29}$$

where

$$(A_{ij},B_{ij},D_{ij},E_{ij},F_{ij},H_{ij})=\int_{-\frac{h}{2}}^{\frac{h}{2}}Q_{ij}(z)\ \ (1,z,z^2,z^3,z^4,z^6)dz$$

$$(A_{ij},D_{ij},F_{ij})=\int_{-\frac{h}{2}}^{\frac{h}{2}}Q_{ij}(z)\ \ (1,z^2,z^4)dz \tag{30}$$

where $i,j=1,2,6$ in the first expression of Eq. (30) and $i,j=4,5$ for the second expression. Here Q_{ij} denote the plane stress material stiffnesses, which are known in terms of the engineering constants as

$$Q_{11}=Q_{22}=\frac{E(z)}{1-\nu^2},\quad Q_{12}=Q_{21}=\frac{\nu E(z)}{1-\nu^2},\quad Q_{66}=G(z)$$

5. Finite element model

5.1. Weak form

The Hamiltons principle or the dynamic version of the principle of virtual displacements of a typical plate finite element is given by

$$0 = \int_{\Omega^e} [N_{xx}\delta u_{,x} + N_{xy}\delta u_{,y}]dxdy - \oint_{\Gamma^e} (\hat{n}_x N_{xx}\delta u + \hat{n}_y N_{xy}\delta u)ds \tag{31}$$

$$0 = \int_{\Omega^e} [N_{xy}\delta v_{,x} + N_{yy}\delta v_{,y}]dxdy - \oint_{\Gamma^e} (\hat{n}_x N_{xy}\delta v + \hat{n}_y N_{yy}\delta v)ds \tag{32}$$

$$\begin{aligned} 0 = \int_{\Omega^e} \Big\{ & \bar{Q}_x\delta w_{,x} + \bar{Q}_y\delta w_{,y} + (N_{xx}w_{,x} + N_{xy}w_{,y})\delta w_{,x} + (N_{xy}w_{,x} + N_{yy}w_{,y})\delta w_{,y} \\ & - c_1(P_{xx}\delta w_{,xx} + P_{yy}\delta w_{,yy} + 2P_{xy}\delta w_{,xy}) - q(1-\mu\nabla^2)\delta w \Big\} dxdy \\ & - \oint_{\Gamma^e} \Big\{ (\bar{Q}_x\hat{n}_x + \bar{Q}_y\hat{n}_y)\delta w + (N_{xx}w_{,x} + N_{xy}w_{,y})\hat{n}_x\delta w + (N_{xy}w_{,x} + N_{yy}w_{,y})\hat{n}_y\delta w \\ & + c_1\Big[P_{xx,x}\hat{n}_x + P_{yy,y}\hat{n}_y + (P_{xy,x}\hat{n}_y + P_{xy,y}\hat{n}_x)\Big]\delta w \\ & - c_1\Big[P_{xx}\delta w_{,x}\hat{n}_x + P_{yy}\delta w_{,y}\hat{n}_y + (P_{xy}\delta w_{,x}\hat{n}_y + P_{xy}\delta w_{,y}\hat{n}_x)\Big]\Big\} ds \end{aligned} \tag{33}$$

$$0 = \int_{\Omega^e} [\bar{Q}_x\delta\phi_x + \bar{M}_{xx}\delta\phi_{x,x} + \bar{M}_{xy}\delta\phi_{x,y}]dxdy - \oint_{\Gamma^e} (M_{xx}\hat{n}_x\delta\phi_x + M_{xy}\hat{n}_y\delta\phi_y)ds \tag{34}$$

$$0 = \int_{\Omega^e} [\bar{Q}_y\delta\phi_x + \bar{M}_{xy}\delta\phi_{x,x} + \bar{M}_{yy}\delta\phi_{x,y}]dxdy - \oint_{\Gamma^e} (M_{xy}\hat{n}_x\delta\phi_x + M_{yy}\hat{n}_y\delta\phi_y)ds \tag{35}$$

5.2. Finite element approximation

In view of the fact that the primary variables of Reddy's third-order theory are

$$u, v, w, \frac{\partial w}{\partial x}, \frac{\partial w}{\partial y}, \frac{\partial^2 w}{\partial x\partial y}, \phi_x, \phi_y$$

we use Lagrange family of approximations to interpolate (u, v, ϕ_x, ϕ_y), while for w we use Hermite family of approximation to interpolate (where the variable and its derivatives are interpolated). We seek finite element approximation in the form

$$u(x,y,t) \approx \sum_{j=1}^{m} U_j(t)\psi_j^{(1)}(x,y) \tag{36}$$

$$v(x,y,t) \approx \sum_{j=1}^{m} V_j(t)\psi_j^{(1)}(x,y) \tag{37}$$

$$w(x,y,t) \approx \sum_{j=1}^{16} \bar{\Delta}_j(t)\varphi_j(x,y) \tag{38}$$

$$\phi_x(x,y,t) \approx \sum_{j=1}^{n} \mathcal{X}_j(t)\psi_j^{(2)}(x,y) \tag{39}$$

$$\phi_y(x,y,t) \approx \sum_{j=1}^{n} \mathcal{Y}_j(t)\psi_j^{(2)}(x,y) \tag{40}$$

Here, $\bar{\Delta}_j$ denote (w, $\partial w/\partial x$, $\partial w/\partial y$, $\partial^2 w/\partial x\partial y$) at each node of a four-node quadrilateral element (known as the conforming element). Substitution of the approximations from Eqs. (36) and (40) into the above weak form Eqs. (31) and (35), we obtain

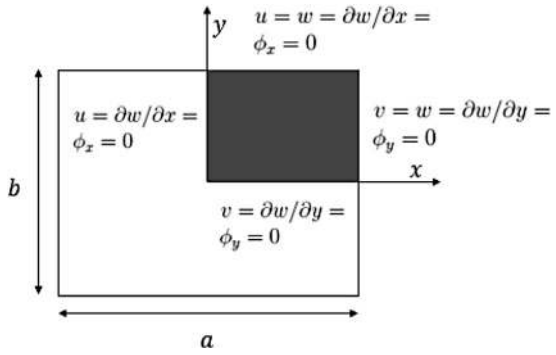

Fig. 1. Boundary conditions and computation domain of simply supported (SS1) plate.

the following finite element equations (for static analysis)

$$\begin{bmatrix} [K^{11}] & [K^{12}] & [K^{13}] & [K^{14}] & [K^{15}] \\ [K^{21}] & [K^{22}] & [K^{23}] & [K^{24}] & [K^{25}] \\ [K^{31}] & [K^{32}] & [K^{33}] & [K^{34}] & [K^{35}] \\ [K^{41}] & [K^{42}] & [K^{43}] & [K^{44}] & [K^{45}] \\ [K^{51}] & [K^{52}] & [K^{53}] & [K^{54}] & [K^{55}] \end{bmatrix} \begin{Bmatrix} \{U\} \\ \{V\} \\ \{\bar{\Delta}\} \\ \{\mathcal{X}\} \\ \{\mathcal{Y}\} \end{Bmatrix} = \begin{Bmatrix} \{F^1\} \\ \{F^2\} \\ \{F^3\} \\ \{F^4\} \\ \{F^5\} \end{Bmatrix}$$

$$K\Delta = F \tag{41}$$

The coefficients of stiffness and force matrices are given in Appendix B

5.3. Solution of nonlinear equations

Solution of Eq. (33) by the Newton iteration method results in the following linearized equations for the incremental solution at the $(r + 1)$st iteration:

$$\delta\Delta = -(\hat{\boldsymbol{T}}(\Delta^r_{s+1}))^{-1}\boldsymbol{R}^r_{s+1} \tag{42}$$

$$\boldsymbol{T}(\Delta^r_{s+1})\left[\frac{\partial \boldsymbol{R}}{\partial \Delta}\right]^r_{s+1}, \quad \boldsymbol{R}^r_{s+1} = \hat{\boldsymbol{K}}(\Delta^r_{s+1})\Delta^r_{s+1} - \hat{\boldsymbol{F}} \tag{43}$$

The total solution is obtained from

$$\Delta^{r+1}_{s+1} = \Delta^r_{s+1} + \delta\Delta \tag{44}$$

The tangent stiffness coefficients are computed and detailed in Appendix C. The following formula given in Reddy (2015), is used to find the tangent stiffness coefficients.

$$T^{\alpha\beta}_{ij} = \frac{\partial R^\alpha_i}{\partial \Delta^\beta_j} = K^{\alpha\beta}_{ij} + \sum_{k=1}^{n_\gamma} \frac{\partial K^{\alpha\gamma}_{ik}}{\partial \Delta^\beta_j}\Delta^\gamma_k - \frac{\partial F^\alpha_i}{\partial \Delta^\beta_j} \tag{45}$$

We note that the von Kármán nonlinearity involves only w or Δ^3. Therefore, only derivatives of $K^{\alpha\beta}$ with respect to Δ^3 are nonzero. Thus, we have to calculate T^{13}_{ij}, T^{23}_{ij}, T^{33}_{ij}, T^{43}_{ij} and T^{53}_{ij}.

6. Numerical results

Numerical results are presented to illustrate the effect of nonlocal parameter μ, power-law index n and the nonlinearity on the bending behavior of functionally graded plates. The boundary conditions considered are simply supported (SS1), as shown in Fig. 1. Because of the symmetry of the problem, the computational domain is taken to be the quadrant depicted in Fig. 1. Four-noded rectangular element with 8 degrees of freedom at each node is used for the analysis. In all the examples, a 4×4 mesh with reduced integration (2×2 rule) for nonlinear terms and shear terms, and a/h ratio of 10 has been considered to obtain plots of the load versus non-dimensional central deflection. The material properties used in computing results are $E_c = 151$ GPa, $E_m = 70$ GPa and $\nu = 0.3$. In all the examples the following non-dimensional parameters are considered. $\bar{w} = \dfrac{w(0,0)}{h}$, $\bar{q} = \dfrac{q_0 a^4}{E_m h^4}$, $\bar{z} = \dfrac{z}{h}$, $\bar{\sigma}_{xx} = \dfrac{\sigma_{xx}(0,0,z)h^2}{q_0 a^2}$

Table 1
Comparison of dimensionless deflections for Al/Zr FGM plate subjected to uniform load ($\bar{q} = 1$) for various power-law index values using rule of mixtures (RM) approach and Mori–Tanaka (MT) scheme.

a/h	$\bar{w}$	n				
		Ceramic	0.5	1	2	Metal
20	Present (RM)	0.02080	0.02657	0.02973	0.03246	0.04486
	Ferreira (RM) (Ferreira et al., 2005)	0.02080	0.0265	0.02970	0.03240	0.04480
	Present (MT)	0.02080	0.02746	0.03052	0.03305	0.04486
	Ferreira (MT) (Ferreira et al., 2005)	0.02080	0.02790	0.03090	0.03330	0.04480
	Qian (MT) (Qian et al., 2004)	0.02118	–	0.03150	0.03395	0.04580
	Difference (%)	0	3.24	2.58	1.78	0
5	Present (RM)	0.02487	0.03148	0.03530	0.03899	0.05366
	Ferreira (RM) (Ferreira et al., 2005)	0.02477	0.03135	0.03515	0.03883	0.05343
	Present (MT)	0.02487	0.03256	0.03634	0.03985	0.05366
	Ferreira (MT) (Ferreira et al., 2005)	0.02477	0.03293	0.03666	0.04009	0.05343
	Qian (MT) (Qian et al., 2004)	0.02436	–	0.03634	0.03976	0.05253
	Difference (%)	0	3.32	2.86	2.15	0

Table 2
Effect of nonlocality on the non-dimensional center deflections of Al/Zr FGM plate subjected to sinusoidal load for various power-law index values.

a/h	n	$\bar{w}$			
		$\mu = 0$	$\mu = 1$	$\mu = 3$	$\mu = 5$
20	Ceramic	0.0132	0.0428	0.1130	0.2159
	0.2	0.0149	0.0483	0.1276	0.2437
	0.5	0.0169	0.0546	0.1443	0.2756
	1	0.0189	0.0611	0.1615	0.3085
	2	0.0207	0.0668	0.1765	0.3372
	Metal	0.0285	0.0922	0.2438	0.4657
10	Ceramic	0.0141	0.0453	0.1193	0.2276
	0.2	0.0158	0.0510	0.1344	0.2565
	0.5	0.0179	0.0576	0.1519	0.2897
	1	0.0201	0.0645	0.1701	0.3245
	2	0.0220	0.0708	0.1866	0.3560
	Metal	0.0304	0.0977	0.2574	0.4910
5	Ceramic	0.0169	0.0538	0.1406	0.2674
	0.2	0.0189	0.0603	0.1577	0.2999
	0.5	0.0213	0.0679	0.1776	0.3378
	1	0.0239	0.0762	0.1993	0.3790
	2	0.0265	0.0844	0.2206	0.4195
	Metal	0.0365	0.1161	0.3034	0.5769

$\bar{\sigma}_{xz} = \dfrac{\sigma_{xz}(0, b/2, z)h^2}{q_0 a^2}$, % difference$= \dfrac{\text{present(MT)}-\text{present(RM)}}{\text{present(MT)}} \times 100$ where a, b, h are the length, breadth and thickness of the plate, respectively, and q_0 is the intensity of the applied load. In all the examples taken below a square plate where $a/b = 1$ is considered.

In Table 1 the non-dimensional central deflections of a simply supported square plate using the rule of mixtures and Mori–Tanaka scheme is calculated and compared with the literature. The presented results are compared well with those computed by the finite point multi-quadric method by Ferreira et al. (2005) (varied by less than 1%). Also the present results are compared well with those results obtained by meshless local Petrov–Galerkin method (MLPG) by Qian et al. (2004) using Mori–Tanaka scheme which shows that the present solution is well matched with the literature and variation is in the range of 1–2%. Table 1 also presents the percentage difference between two homogenization schemes with respect to Mori–Tanaka scheme and it is evident that for power-law index $n = 0$ and $n = \infty$ both yield exact same value of deflection, as in both of these schemes for $n = 0$ and $n = \infty$, material properties reduce to ceramic and metal, respectively. It is shown by Qian et al. (2004) that the MLPG solution agreed very well with the exact solution of Vel and Batra (2002). It is observed that the percentage difference between the deflection values corresponding to a/h ratio of 5 and 20 is maximum at the power index value of 0.5. Although rule of mixtures is a simple arithmetic average, whereas Mori–Tanaka scheme takes into account the interaction of the elastic fields between neighboring inclusions (Vel & Batra, 2002), in the following examples we used the rule of mixtures approach for its simple nature and also we believe it is reasonable in predicting the global responses (Shen & Wang, 2012). Table 2 shows the effect of nonlocal parameter on non-dimensional center deflections. The deflections are increasing with the increase in the nonlocal parameter μ irrespective of any power-law index n and the a/h ratio.

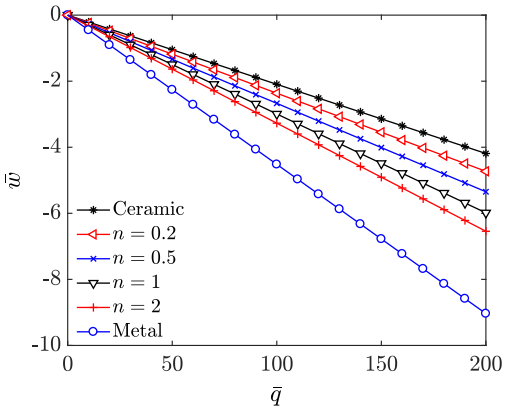

Fig. 2. Non-dimensional center deflection versus load parameter for various values of power-law index n; uniform load and linear analysis ($\mu = 0$).

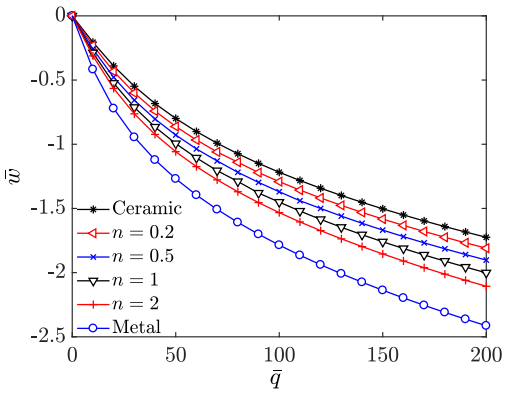

Fig. 3. Non-dimensional center deflection versus load parameter for various values of power-law index n; uniform load and nonlinear analysis ($\mu = 0$).

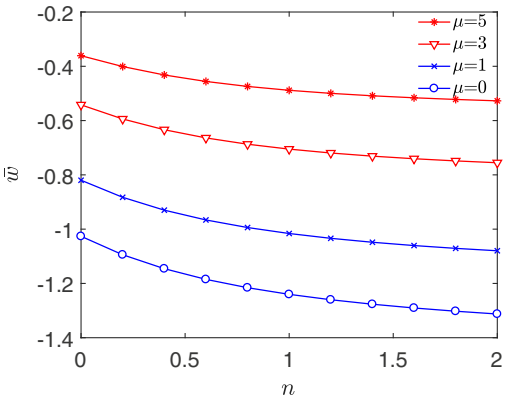

Fig. 4. Non-dimensional center deflection versus power-law index for various values of μ; sinusoidal load and nonlinear analysis.

In Fig. 2 plots of the linear non-dimensional center deflections versus load for different values of the power-law index is presented. As the metal plate ($n \to \infty$) has lower stiffness compared to the ceramic plate ($n = 0$), it is expected to deflect more than the ceramic plate; and for all other intermediate values of n, the deflections increase with increase in n. Fig. 3 contains plots of nonlinear non-dimensional center deflection versus load for different values of the power-law index. To show the effect of nonlinearity the deflections are plotted up to a very high value of load ($\bar{q} = 200$). The deflections are becoming completely nonlinear for a value of $\bar{q}$ greater than 50 for all the power-law index values. Fig. 4 shows the variation of nonlinear non-dimensional deflections with n and μ values. The non-dimensional deflection increases with an increase in the power-law index value and percentage difference between extreme values is about 20–40%. From Fig. 5, it is observed that for a fixed power-law index, an increase in the nonlocal parameter results in an increase in deflections, as expected because of a reduction in the stiffness. If we consider the first three curves in Fig. 5, which have the same power-law

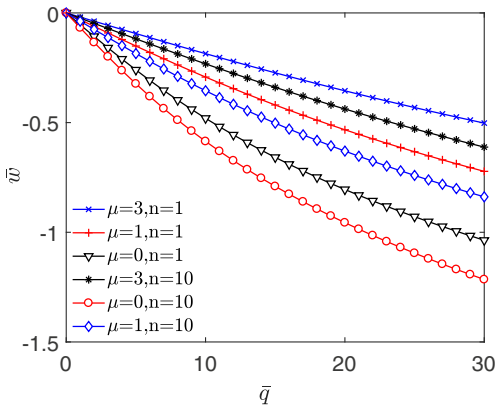

Fig. 5. Non-dimensional center deflection versus load parameter for various values of μ and n; sinusoidal load and nonlinear analysis.

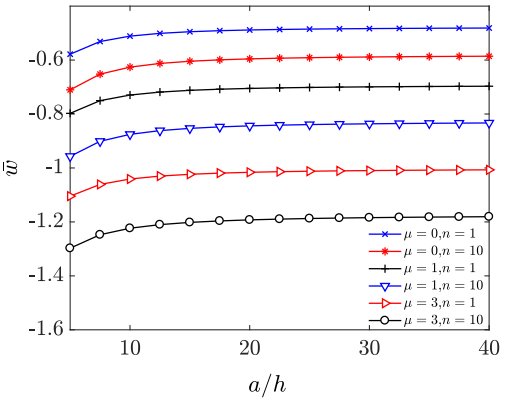

Fig. 6. Non-dimensional center deflection versus a/h ratio for various values of μ and n; sinusoidal load and nonlinear analysis.

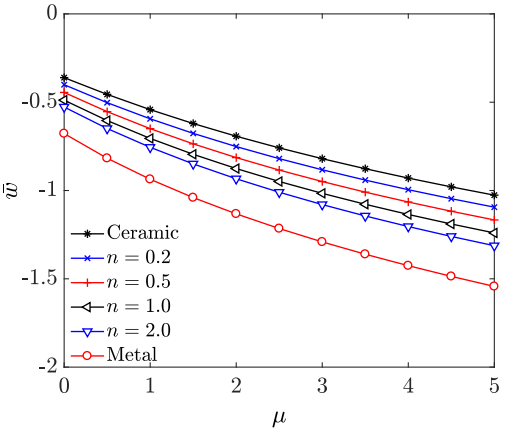

Fig. 7. Non-dimensional center deflection versus μ for various values of power-law index n; sinusoidal load and nonlinear analysis.

index value i.e. $n = 1$ the deflections are increasing significantly with an increase in the value of μ from 1 to 3 and to 5. This indicates that Eringen's stress gradient model is a diffusion type model and has the effect of representing the plate as flexible. In Fig. 6, the effect of a/h ratio on the non-dimensional center deflections is shown. It can be observed that there is an increase in the deflections from a/h ratio 5 to 10 after which it is almost constant. With the increase in the nonlocal parameter the deflections increase nonlinearly and a similar trend is observed for various values of the power-law index, as shown in Fig. 7.

The bending stress $\bar{\sigma}_{xx}$ and the transverse shear stress $\bar{\sigma}_{xz}$ are computed at the center of the plate and at the unconstrained corners of the plate, respectively. The bending stresses of the TSDT do not differ much from the bending stresses

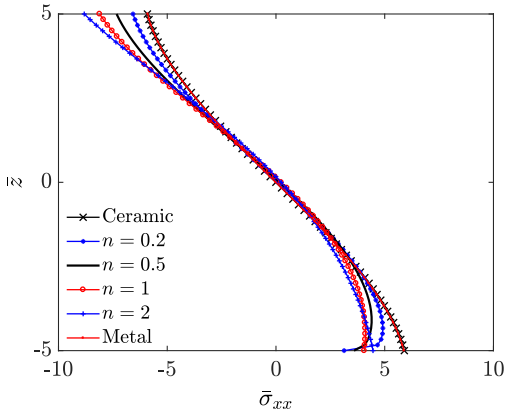

Fig. 8. Bending stress versus $\bar{z}$ for various values of power-law index n; uniform load and nonlinear analysis.

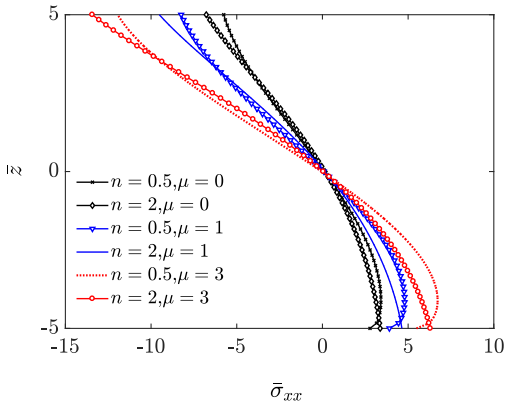

Fig. 9. Bending stress versus $\bar{z}$ for various values of power-law index n and nonlocal parameter μ; sinusoidal load and nonlinear analysis.

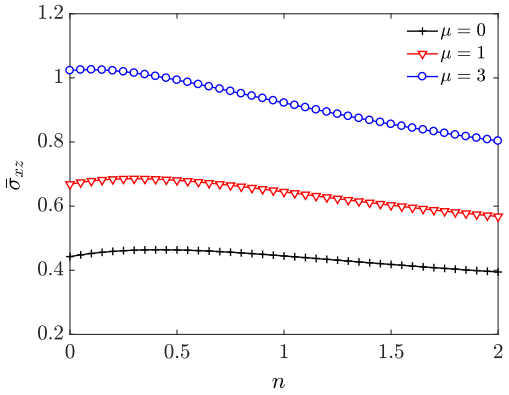

Fig. 10. Transverse shear stress versus power-law index n for various values of the nonlocal parameter μ; sinusoidal load and nonlinear analysis.

of the FSDT (Vel & Batra, 2002). The nonlinear stress variation of TSDT for various values of the power-law index under uniform load, is given in Fig. 8. The bending stresses are varying nonlinearly through the thickness even for the extreme values of power-law index. The steep gradients of some curves in the bending stress plot near the bottom of the plate are due to sudden change in the material properties at that point of the plate. Fig. 9 shows the effect of nonlocal parameter on the bending stresses through the thickness of the plate. With a fixed value of non local parameter μ , values of the stresses decrease with increase in the n value. Fig. 10 shows a plot of the transverse shear stress versus power index for various values of the nonlocal parameter. From Fig. 10, it is clear that the transverse shear stress is maximum at some points in between $n = 0$ and $n = 0.5$. The transverse shear stresses are almost constant or the rate of decrease is becoming minimum as we increase the power-law index value.

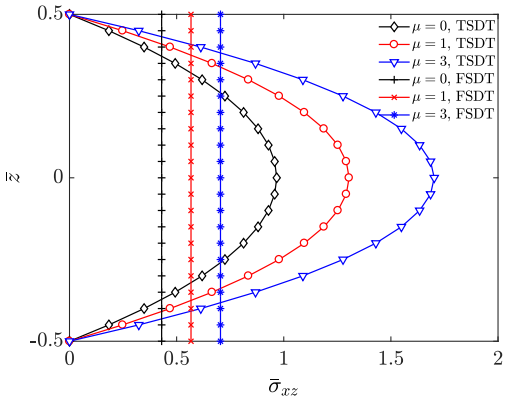

Fig. 11. Transverse shear stress through the thickness for various values of the nonlocal parameter μ by TSDT and FSDT; sinusoidal load and nonlinear analysis.

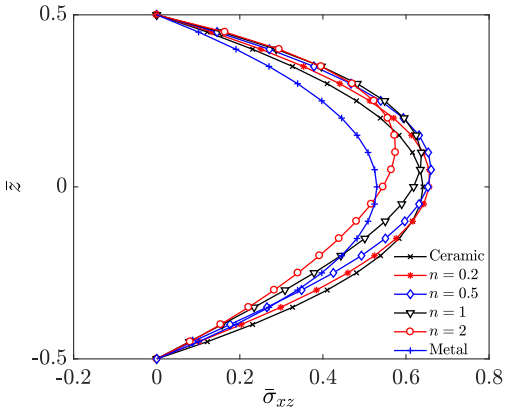

Fig. 12. Transverse shear stress through the thickness for various values of the power-law index n; uniform load and nonlinear analysis.

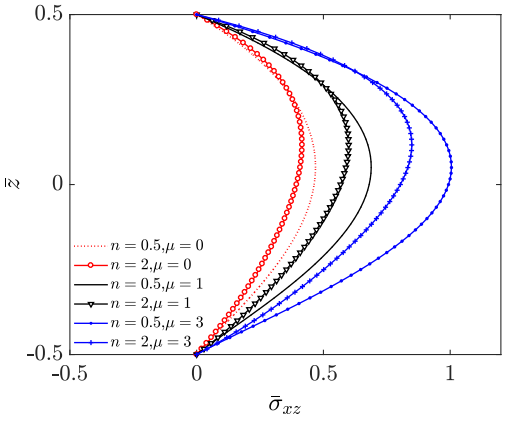

Fig. 13. Transverse shear stress through the thickness for various values of the nonlocal parameter μ and the power-law index n; sinusoidal load and nonlinear analysis.

The variation of transverse shear strains of the TSDT is quadratic through the thickness; therefore, the transverse shear stresses will also vary quadratically. From Fig. 11 it is clear that for TSDT the shear stress has a quadratic variation, whereas in FSDT it is a constant. From Fig. 11 we can see that the transverse shear stresses are increasing with the increase of nonlocal parameter in both the theories. Unlike for the homogeneous plate, the variation of the stresses of the FGM plate depends not only on the variation of strains, but also in the variation of the material properties in the plate. Fig. 12 shows the transverse shear stress variation through the thickness and for various values of the power-law index n for the case of uniform load. From the plot we can see that, transverse shear stress goes to zero at top and bottom surfaces and varies

quadratically through the thickness. The peak in the transverse shear stress is not exactly at the mid plane except for the extreme cases (i.e. for ceramic and metal). In all other cases the maximum value occurs at the neutral plane, which depends on power-law index and volume fraction of the components of the plate. Fig. 13 shows the variation of transverse shear stress through the thickness with various values of μ and n. Fig. 13 shows that transverse shear stresses increase with the increase in the nonlocal parameter.

7. Conclusions

Equations of equilibrium of Reddy's third-order shear deformation theory for the analysis of FGM plates are derived based on Eringen's nonlocal differential constitutive model and the von Kármán nonlinear strains. The weak forms are derived and the finite element model is developed. Numerical examples are presented to bring out the parametric effect such as the power-index, non-local parameters, and side-to-thickness ratio a/h and the von Kármán nonlinearity on the bending behavior of FGM plates. It has been observed that the Eringen's nonlocal model results in reduced structural stiffness of FGM plates, hence the deflections increase with the nonlocal parameter.

Appendix A

The governing equations of equilibrium for the bending of plates based on the nonlinear third-order shear deformable plate theory are

$$\frac{\partial N_{xx}^{nl}}{\partial x}+\frac{\partial N_{xy}^{nl}}{\partial y}=0$$

$$\frac{\partial N_{xy}^{nl}}{\partial x}+\frac{\partial N_{yy}^{nl}}{\partial y}=0$$

$$\frac{\partial \bar{Q}_{x}^{nl}}{\partial x}+\frac{\partial \bar{Q}_{y}^{nl}}{\partial y}+\frac{\partial}{\partial x}\left(N_{xx}^{nl}\frac{\partial w}{\partial x}+N_{xy}^{nl}\frac{\partial w}{\partial y}\right)+\frac{\partial}{\partial y}\left(N_{xy}^{nl}\frac{\partial w}{\partial x}+N_{yy}^{nl}\frac{\partial w}{\partial y}\right)$$

$$+c_1\left(\frac{\partial^2 P_{xx}^{nl}}{\partial x^2}+2\frac{\partial^2 P_{xy}^{nl}}{\partial x\partial y}+\frac{\partial^2 P_{yy}^{nl}}{\partial y^2}\right)+q=0$$

$$\frac{\partial \bar{M}_{xx}^{nl}}{\partial x}+\frac{\partial \bar{M}_{xy}^{nl}}{\partial y}-\bar{Q}_{x}^{nl}=0$$

$$\frac{\partial \bar{M}_{xy}^{nl}}{\partial x}+\frac{\partial \bar{M}_{yy}^{nl}}{\partial y}-\bar{Q}_{y}^{nl}=0$$

where

$$\bar{M}_{\alpha\beta}^{nl}=M_{\alpha\beta}^{nl}-c_1P_{\alpha\beta}^{nl},\quad \bar{Q}_{\alpha}^{nl}=Q_{\alpha}^{nl}-c_2R_{\alpha}^{nl}$$

The relation between local and nonlocal stress resultants can be derived from Eq. (8) as

$$\mathcal{L}(N_{\alpha\beta}^{nl})=N_{\alpha\beta}^{nl},\quad \mathcal{L}(M_{\alpha\beta}^{nl})=M_{\alpha\beta}^{nl},\quad \mathcal{L}(P_{\alpha\beta}^{nl})=P_{\alpha\beta}^{nl},\quad \mathcal{L}(Q_{\alpha}^{nl})=Q_{\alpha}^{nl},\quad \mathcal{L}(R_{\alpha}^{nl})=R_{\alpha}^{nl}$$

Appendix B

Stiffness matrix term's

$$K_{ij}^{11}=\int_{\Omega^e}\left[A_{11}\frac{\partial\psi_j^{(1)}}{\partial x}\frac{\partial\psi_i^{(1)}}{\partial x}+A_{66}\frac{\partial\psi_j^{(1)}}{\partial y}\frac{\partial\psi_i^{(1)}}{\partial y}+A_{16}\left(\frac{\partial\psi_j^{(1)}}{\partial y}\frac{\partial\psi_i^{(1)}}{\partial x}+\frac{\partial\psi_i^{(1)}}{\partial y}\frac{\partial\psi_j^{(1)}}{\partial x}\right)\right]dxdy$$

$$K_{ij}^{12}=\int_{\Omega^e}\left[A_{12}\frac{\partial\psi_i^{(1)}}{\partial x}\frac{\partial\psi_j^{(1)}}{\partial y}+A_{16}\frac{\partial\psi_i^{(1)}}{\partial x}\frac{\partial\psi_j^{(1)}}{\partial x}+A_{66}\frac{\partial\psi_i^{(1)}}{\partial y}\frac{\partial\psi_j^{(1)}}{\partial x}+A_{26}\frac{\partial\psi_i^{(1)}}{\partial y}\frac{\partial\psi_j^{(1)}}{\partial y}\right]dxdy$$

$$\begin{aligned}K_{ij}^{13}=\int_{\Omega^e}\Bigg\{&\frac{\partial\psi_i^{(1)}}{\partial x}\left[\frac{1}{2}A_{11}\frac{\partial w}{\partial x}\frac{\partial\varphi_j}{\partial x}+\frac{1}{2}A_{12}\frac{\partial w}{\partial y}\frac{\partial\varphi_j}{\partial y}+\frac{1}{2}A_{16}\left(\frac{\partial w}{\partial x}\frac{\partial\varphi_j}{\partial y}+\frac{\partial w}{\partial y}\frac{\partial\varphi_j}{\partial x}\right)\right.\\&\left.-c_1E_{11}\frac{\partial^2\varphi_j}{\partial x^2}-c_1E_{12}\frac{\partial^2\varphi_j}{\partial y^2}-2c_1E_{16}\frac{\partial^2\varphi_j}{\partial x\partial y}\right)+\frac{\partial\psi_i^{(1)}}{\partial y}\left[\frac{1}{2}A_{16}\frac{\partial w}{\partial x}\frac{\partial\varphi_j}{\partial x}+\frac{1}{2}A_{26}\frac{\partial w}{\partial y}\frac{\partial\varphi_j}{\partial y}\right.\\&\left.+\frac{1}{2}A_{66}\left(\frac{\partial w}{\partial x}\frac{\partial\varphi_j}{\partial y}+\frac{\partial w}{\partial y}\frac{\partial\varphi_j}{\partial x}\right)-c_1E_{16}\frac{\partial^2\varphi_j}{\partial x^2}-c_1E_{26}\frac{\partial^2\varphi_j}{\partial y^2}-2c_1E_{66}\frac{\partial^2\varphi_j}{\partial x\partial y}\right]\Bigg\}dxdy\end{aligned}$$

$$K_{ij}^{14} = \int_{\Omega^e} \left\{ \frac{\partial \psi_i^{(1)}}{\partial x} \left[(B_{11} - c_1 E_{11}) \frac{\partial \psi_j^{(2)}}{\partial x} + (B_{16} - c_1 E_{16}) \frac{\partial \psi_j^{(2)}}{\partial y} \right] + \frac{\partial \psi_i^{(1)}}{\partial y} \left[(B_{16} - c_1 E_{16}) \frac{\partial \psi_j^{(2)}}{\partial x} + (B_{66} - c_1 E_{66}) \frac{\partial \psi_j^{(2)}}{\partial y} \right] \right\} dxdy$$

$$K_{ij}^{15} = \int_{\Omega^e} \left\{ \frac{\partial \psi_i^{(1)}}{\partial x} \left[(B_{16} - c_1 E_{16}) \frac{\partial \psi_j^{(2)}}{\partial x} + (B_{12} - c_1 E_{12}) \frac{\partial \psi_j^{(2)}}{\partial y} \right] + \frac{\partial \psi_i^{(1)}}{\partial y} \left[(B_{66} - c_1 E_{66}) \frac{\partial \psi_j^{(2)}}{\partial x} + (B_{26} - c_1 E_{26}) \frac{\partial \psi_j^{(2)}}{\partial y} \right] \right\} dxdy$$

$$K_{ij}^{21} = \int_{\Omega^e} \left[A_{16} \frac{\partial \psi_j^{(1)}}{\partial x} \frac{\partial \psi_i^{(1)}}{\partial x} + A_{66} \frac{\partial \psi_i^{(1)}}{\partial x} \frac{\partial \psi_j^{(1)}}{\partial y} + A_{12} \frac{\partial \psi_i^{(1)}}{\partial y} \frac{\partial \psi_j^{(1)}}{\partial x} + A_{26} \frac{\partial \psi_i^{(1)}}{\partial y} \frac{\partial \psi_j^{(1)}}{\partial y} \right) \right] dxdy$$

$$K_{ij}^{22} = \int_{\Omega^e} \left[A_{66} \frac{\partial \psi_i^{(1)}}{\partial x} \frac{\partial \psi_j^{(1)}}{\partial x} + A_{22} \frac{\partial \psi_i^{(1)}}{\partial y} \frac{\partial \psi_j^{(1)}}{\partial y} + A_{26} \left(\frac{\partial \psi_i^{(1)}}{\partial y} \frac{\partial \psi_j^{(1)}}{\partial x} + \frac{\partial \psi_i^{(1)}}{\partial x} \frac{\partial \psi_j^{(1)}}{\partial y} \right) \right] dxdy$$

$$K_{ij}^{23} = \int_{\Omega^e} \left\{ \frac{\partial \psi_i^{(1)}}{\partial x} \left[\frac{1}{2} A_{16} \frac{\partial w}{\partial x} \frac{\partial \varphi_j}{\partial x} + \frac{1}{2} A_{26} \frac{\partial w}{\partial y} \frac{\partial \varphi_j}{\partial y} + \frac{1}{2} A_{66} \left(\frac{\partial w}{\partial x} \frac{\partial \varphi_j}{\partial y} + \frac{\partial w}{\partial y} \frac{\partial \varphi_j}{\partial x} \right) - c_1 E_{16} \frac{\partial^2 \varphi_j}{\partial x^2} - c_1 E_{26} \frac{\partial^2 \varphi_j}{\partial y^2} - 2 c_1 E_{66} \frac{\partial^2 \varphi_j}{\partial x \partial y} \right) + \frac{\partial \psi_i^{(1)}}{\partial y} \left[\frac{1}{2} A_{12} \frac{\partial w}{\partial x} \frac{\partial \varphi_j}{\partial x} + \frac{1}{2} A_{22} \frac{\partial w}{\partial y} \frac{\partial \varphi_j}{\partial y} + \frac{1}{2} A_{26} \left(\frac{\partial w}{\partial x} \frac{\partial \varphi_j}{\partial y} + \frac{\partial w}{\partial y} \frac{\partial \varphi_j}{\partial x} \right) - c_1 E_{12} \frac{\partial^2 \varphi_j}{\partial x^2} - c_1 E_{22} \frac{\partial^2 \varphi_j}{\partial y^2} - 2 c_1 E_{26} \frac{\partial^2 \varphi_j}{\partial x \partial y} \right] \right\} dxdy$$

$$K_{ij}^{24} = \int_{\Omega^e} \left\{ \frac{\partial \psi_i^{(1)}}{\partial x} \left[(B_{16} - c_1 E_{16}) \frac{\partial \psi_j^{(2)}}{\partial x} + (B_{66} - c_1 E_{66}) \frac{\partial \psi_j^{(2)}}{\partial y} \right] + \frac{\partial \psi_i^{(1)}}{\partial y} \left[(B_{12} - c_1 E_{12}) \frac{\partial \psi_j^{(2)}}{\partial x} + (B_{26} - c_1 E_{26}) \frac{\partial \psi_j^{(2)}}{\partial y} \right] \right\} dxdy$$

$$K_{ij}^{25} = \int_{\Omega^e} \left\{ \frac{\partial \psi_i^{(1)}}{\partial x} \left[(B_{66} - c_1 E_{66}) \frac{\partial \psi_j^{(2)}}{\partial x} + (B_{26} - c_1 E_{26}) \frac{\partial \psi_j^{(2)}}{\partial y} \right] + \frac{\partial \psi_i^{(1)}}{\partial y} \left[(B_{26} - c_1 E_{26}) \frac{\partial \psi_j^{(2)}}{\partial x} + (B_{22} - c_1 E_{22}) \frac{\partial \psi_j^{(2)}}{\partial y} \right] \right\} dxdy$$

$$K_{ij}^{31} = \int_{\Omega^e} \left[\frac{\partial \varphi_i}{\partial x} \left(A_{11} \frac{\partial w}{\partial x} \frac{\partial \psi_j^{(1)}}{\partial x} + A_{16} \frac{\partial w}{\partial x} \frac{\partial \psi_j^{(1)}}{\partial y} + A_{16} \frac{\partial w}{\partial y} \frac{\partial \psi_j^{(1)}}{\partial x} + A_{66} \frac{\partial w}{\partial y} \frac{\partial \psi_j^{(1)}}{\partial y} \right) + \frac{\partial \varphi_i}{\partial y} \left(A_{16} \frac{\partial w}{\partial x} \frac{\partial \psi_j^{(1)}}{\partial x} + A_{66} \frac{\partial w}{\partial x} \frac{\partial \psi_j^{(1)}}{\partial y} + A_{12} \frac{\partial w}{\partial y} \frac{\partial \psi_j^{(1)}}{\partial x} + A_{26} \frac{\partial w}{\partial y} \frac{\partial \psi_j^{(1)}}{\partial y} \right) + \left(- c_1 E_{11} \frac{\partial \psi_j^{(1)}}{\partial x} \frac{\partial^2 \varphi_i}{\partial x^2} - c_1 E_{16} \frac{\partial \psi_j^{(1)}}{\partial y} \frac{\partial^2 \varphi_i}{\partial x^2} - c_1 E_{12} \frac{\partial \psi_j^{(1)}}{\partial x} \frac{\partial^2 \varphi_i}{\partial y^2} - c_1 E_{26} \frac{\partial \psi_j^{(1)}}{\partial y} \frac{\partial^2 \varphi_i}{\partial y^2} - 2 c_1 E_{16} \frac{\partial \psi_j^{(1)}}{\partial x} \frac{\partial^2 \varphi_i}{\partial x \partial y} - 2 c_1 E_{66} \frac{\partial \psi_j^{(1)}}{\partial y} \frac{\partial^2 \varphi_i}{\partial x \partial y} \right) \right] dxdy$$

$$K_{ij}^{32} = \int_{\Omega^e} \left[\frac{\partial \varphi_i}{\partial x} \left(A_{12} \frac{\partial w}{\partial x} \frac{\partial \psi_j^{(1)}}{\partial y} + A_{16} \frac{\partial w}{\partial x} \frac{\partial \psi_j^{(1)}}{\partial x} + A_{26} \frac{\partial w}{\partial y} \frac{\partial \psi_j^{(1)}}{\partial y} + A_{66} \frac{\partial w}{\partial y} \frac{\partial \psi_j^{(1)}}{\partial x} \right) + \frac{\partial \varphi_i}{\partial y} \left(A_{26} \frac{\partial w}{\partial x} \frac{\partial \psi_j^{(1)}}{\partial y} + A_{66} \frac{\partial w}{\partial x} \frac{\partial \psi_j^{(1)}}{\partial x} + A_{22} \frac{\partial w}{\partial y} \frac{\partial \psi_j^{(1)}}{\partial y} + A_{26} \frac{\partial w}{\partial y} \frac{\partial \psi_j^{(1)}}{\partial x} \right) + \left(- c_1 E_{12} \frac{\partial \psi_j^{(1)}}{\partial y} \frac{\partial^2 \varphi_i}{\partial x^2} - c_1 E_{16} \frac{\partial \psi_j^{(1)}}{\partial x} \frac{\partial^2 \varphi_i}{\partial x^2} - c_1 E_{22} \frac{\partial \psi_j^{(1)}}{\partial y} \frac{\partial^2 \varphi_i}{\partial y^2} - c_1 E_{26} \frac{\partial \psi_j^{(1)}}{\partial x} \frac{\partial^2 \varphi_i}{\partial y^2} - 2 c_1 E_{26} \frac{\partial \psi_j^{(1)}}{\partial y} \frac{\partial^2 \varphi_i}{\partial x \partial y} - 2 c_1 E_{66} \frac{\partial \psi_j^{(1)}}{\partial x} \frac{\partial^2 \varphi_i}{\partial x \partial y} \right) \right] dxdy$$

$$K_{ij}^{33} = \int_{\Omega^e} \left[\frac{\partial \varphi_i}{\partial x} \left(A_{55} \frac{\partial \varphi_j}{\partial x} - 2 c_2 D_{55} \frac{\partial \varphi_j}{\partial x} + c_2^2 F_{55} \frac{\partial \varphi_j}{\partial x} + A_{45} \frac{\partial \varphi_j}{\partial y} - 2 c_2 D_{45} \frac{\partial \varphi_j}{\partial y} + c_2^2 F_{45} \frac{\partial \varphi_j}{\partial y} \right) + \frac{\partial \varphi_i}{\partial y} \left(A_{44} \frac{\partial \varphi_j}{\partial y} - 2 c_2 D_{44} \frac{\partial \varphi_j}{\partial y} + c_2^2 F_{44} \frac{\partial \varphi_j}{\partial y} + A_{45} \frac{\partial \varphi_j}{\partial x} - 2 c_2 D_{45} \frac{\partial \varphi_j}{\partial x} + c_2^2 F_{45} \frac{\partial \varphi_j}{\partial x} \right)$$

$$
\begin{aligned}
&+\left(\frac{1}{2}A_{11}\left(\frac{\partial w}{\partial x}\right)^2+\frac{1}{2}A_{12}\left(\frac{\partial w}{\partial y}\right)^2+A_{16}\frac{\partial w}{\partial x}\frac{\partial w}{\partial y}\right)\frac{\partial\varphi_i}{\partial x}\frac{\partial\varphi_j}{\partial x}\\
&+\left(\frac{1}{2}A_{16}\left(\frac{\partial w}{\partial x}\right)^2+\frac{1}{2}A_{26}\left(\frac{\partial w}{\partial y}\right)^2+A_{66}\frac{\partial w}{\partial x}\frac{\partial w}{\partial y}\right)\left(\frac{\partial\varphi_i}{\partial x}\frac{\partial\varphi_j}{\partial y}+\frac{\partial\varphi_i}{\partial y}\frac{\partial\varphi_j}{\partial x}\right)\\
&+\left(\frac{1}{2}A_{12}\left(\frac{\partial w}{\partial x}\right)^2+\frac{1}{2}A_{22}\left(\frac{\partial w}{\partial y}\right)^2+A_{26}\frac{\partial w}{\partial x}\frac{\partial w}{\partial y}\right)\frac{\partial\varphi_i}{\partial y}\frac{\partial\varphi_j}{\partial y}\\
&+\frac{\partial\varphi_i}{\partial x}\Big(-c_1E_{11}\frac{\partial w}{\partial x}\frac{\partial^2\varphi_j}{\partial x^2}-c_1E_{12}\frac{\partial w}{\partial x}\frac{\partial^2\varphi_j}{\partial y^2}-2c_1E_{16}\frac{\partial w}{\partial x}\frac{\partial\varphi_j}{\partial x\partial y}\\
&-c_1E_{16}\frac{\partial w}{\partial y}\frac{\partial^2\varphi_j}{\partial x^2}-c_1E_{26}\frac{\partial w}{\partial y}\frac{\partial^2\varphi_j}{\partial y^2}-2c_1E_{66}\frac{\partial w}{\partial y}\frac{\partial\varphi_j}{\partial x\partial y}\Big)\\
&+\frac{\partial\varphi_i}{\partial y}\Big(-c_1E_{16}\frac{\partial w}{\partial x}\frac{\partial^2\varphi_j}{\partial x^2}-c_1E_{26}\frac{\partial w}{\partial x}\frac{\partial^2\varphi_j}{\partial y^2}-2c_1E_{66}\frac{\partial w}{\partial x}\frac{\partial\varphi_j}{\partial x\partial y}\\
&-c_1E_{12}\frac{\partial w}{\partial y}\frac{\partial^2\varphi_j}{\partial x^2}-c_1E_{22}\frac{\partial w}{\partial y}\frac{\partial^2\varphi_j}{\partial y^2}-2c_1E_{26}\frac{\partial w}{\partial y}\frac{\partial\varphi_j}{\partial x\partial y}\Big)\\
&+\frac{\partial^2\varphi_i}{\partial x^2}\Big(-\frac{1}{2}c_1E_{11}\frac{\partial w}{\partial x}\frac{\partial\varphi_j}{\partial x}-\frac{1}{2}c_1E_{12}\frac{\partial w}{\partial y}\frac{\partial\varphi_j}{\partial y}+\frac{1}{2}c_1E_{16}\Big(\frac{\partial w}{\partial x}\frac{\partial\varphi_j}{\partial y}+\frac{\partial w}{\partial y}\frac{\partial\varphi_j}{\partial x}\Big)\\
&+c_1^2H_{11}\frac{\partial^2\varphi_j}{\partial x^2}+c_1^2H_{12}\frac{\partial^2\varphi_j}{\partial y^2}+2c_1^2H_{16}\frac{\partial^2 w}{\partial x\partial y}\Big)+\frac{\partial^2\varphi_i}{\partial y^2}\Big(-\frac{1}{2}c_1E_{12}\frac{\partial w}{\partial x}\frac{\partial\varphi_j}{\partial x}\\
&-\frac{1}{2}c_1E_{22}\frac{\partial w}{\partial y}\frac{\partial\varphi_j}{\partial y}+\frac{1}{2}c_1E_{26}\Big(\frac{\partial w}{\partial x}\frac{\partial\varphi_j}{\partial y}+\frac{\partial w}{\partial y}\frac{\partial\varphi_j}{\partial x}\Big)+c_1^2H_{12}\frac{\partial^2\varphi_j}{\partial x^2}+c_1^2H_{22}\frac{\partial^2\varphi_j}{\partial y^2}\\
&+2c_1^2H_{26}\frac{\partial^2\varphi_j}{\partial x\partial y}\Big)+\frac{\partial^2\varphi_i}{\partial x\partial y}\Big(-c_1E_{16}\frac{\partial w}{\partial x}\frac{\partial\varphi_j}{\partial x}-c_1E_{26}\frac{\partial w}{\partial y}\frac{\partial\varphi_j}{\partial y}\\
&-c_1E_{66}\Big(\frac{\partial w}{\partial x}\frac{\partial\varphi_j}{\partial y}+\frac{\partial w}{\partial y}\frac{\partial\varphi_j}{\partial x}\Big)+2c_1H_{16}\frac{\partial^2\varphi_j}{\partial x^2}+2c_1H_{26}\frac{\partial^2\varphi_j}{\partial y^2}+4c_1^2H_{66}\frac{\partial^2\varphi_j}{\partial x\partial y}\Big)\Big]dxdy
\end{aligned}
$$

$$
\begin{aligned}
K_{ij}^{34}=\int_{\Omega^e}\Big\{&\frac{\partial\varphi_i}{\partial x}\Big[(A_{55}-2c_2D_{55}+c_2^2F_{55})\psi_j^{(2)}+(B_{16}-c_1E_{16})\frac{\partial\psi_j^{(2)}}{\partial x}\frac{\partial w}{\partial y}\\
&+(B_{66}-c_1E_{66})\frac{\partial\psi_j^{(2)}}{\partial y}\frac{\partial w}{\partial y}+(B_{11}-c_1E_{11})\frac{\partial\psi_j^{(2)}}{\partial x}\frac{\partial w}{\partial x}+(B_{16}-c_1E_{16})\frac{\partial\psi_j^{(2)}}{\partial y}\frac{\partial w}{\partial x}\Big]\\
&+\frac{\partial\varphi_i}{\partial y}\Big[(A_{45}-2c_2D_{45}+c_2^2F_{45})\psi_j^{(2)}+(B_{66}-c_1E_{66})\frac{\partial\psi_j^{(2)}}{\partial y}\frac{\partial w}{\partial x}+(B_{16}-c_1E_{16})\frac{\partial\psi_j^{(2)}}{\partial x}\frac{\partial w}{\partial x}\\
&+(B_{12}-c_1E_{12})\frac{\partial\psi_j^{(2)}}{\partial x}\frac{\partial w}{\partial y}+(B_{26}-c_1E_{26})\frac{\partial\psi_j^{(2)}}{\partial y}\frac{\partial w}{\partial y}\Big]+\frac{\partial^2\varphi_i}{\partial x^2}\Big[-c_1F_{11}\frac{\partial\psi_j^{(2)}}{\partial x}\\
&-c_1F_{16}\frac{\partial\psi_j^{(2)}}{\partial y}+c_1^2H_{11}\frac{\partial\psi_j^{(2)}}{\partial x}+c_1^2H_{16}\frac{\partial\psi_j^{(2)}}{\partial y}\Big]+\frac{\partial^2\varphi_i}{\partial y^2}\Big[-c_1F_{12}\frac{\partial\psi_j^{(2)}}{\partial x}-c_1F_{26}\frac{\partial\psi_j^{(2)}}{\partial y}+c_1^2H_{12}\frac{\partial\psi_j^{(2)}}{\partial x}\\
&+c_1^2H_{26}\frac{\partial\psi_j^{(2)}}{\partial y}\Big]+\frac{\partial^2\varphi_i}{\partial x\partial y}\Big[-2c_1F_{16}\frac{\partial\psi_j^{(2)}}{\partial x}-2c_1F_{66}\frac{\partial\psi_j^{(2)}}{\partial y}+2c_1^2H_{16}\frac{\partial\psi_j^{(2)}}{\partial x}+2c_1^2H_{66}\frac{\partial\psi_j^{(2)}}{\partial y}\Big]\Big\}dxdy
\end{aligned}
$$

$$
\begin{aligned}
K_{ij}^{35}=\int_{\Omega^e}\Big\{&\frac{\partial\varphi_i}{\partial x}\Big[(A_{45}-2c_2D_{45}+c_2^2F_{45})\psi_j^{(2)}+(B_{12}-c_1E_{12})\frac{\partial\psi_j^{(2)}}{\partial y}\frac{\partial w}{\partial x}\\
&+(B_{16}-c_1E_{16})\frac{\partial\psi_j^{(2)}}{\partial x}\frac{\partial w}{\partial x}+(B_{26}-c_1E_{26})\frac{\partial\psi_j^{(2)}}{\partial y}\frac{\partial w}{\partial y}+(B_{66}-c_1E_{66})\frac{\partial\psi_j^{(2)}}{\partial x}\frac{\partial w}{\partial y}\Big]\\
&+\frac{\partial\varphi_i}{\partial y}\Big[(A_{44}-2c_2D_{44}+c_2^2F_{44})\psi_j^{(2)}+(B_{26}-c_1E_{26})\frac{\partial\psi_j^{(2)}}{\partial y}\frac{\partial w}{\partial x}+(B_{66}-c_1E_{66})\frac{\partial\psi_j^{(2)}}{\partial x}\frac{\partial w}{\partial x}\\
&+(B_{22}-c_1E_{22})\frac{\partial\psi_j^{(2)}}{\partial y}\frac{\partial w}{\partial y}+(B_{26}-c_1E_{26})\frac{\partial\psi_j^{(2)}}{\partial x}\frac{\partial w}{\partial y}\Big]+\frac{\partial^2\varphi_i}{\partial x^2}\Big[-c_1F_{12}\frac{\partial\psi_j^{(2)}}{\partial y}\\
&-c_1F_{16}\frac{\partial\psi_j^{(2)}}{\partial x}+c_1^2H_{12}\frac{\partial\psi_j^{(2)}}{\partial y}+c_1^2H_{16}\frac{\partial\psi_j^{(2)}}{\partial x}\Big]+\frac{\partial^2\varphi_i}{\partial y^2}\Big[-c_1F_{22}\frac{\partial\psi_j^{(2)}}{\partial y}-c_1F_{26}\frac{\partial\psi_j^{(2)}}{\partial x}+c_1^2H_{22}\frac{\partial\psi_j^{(2)}}{\partial y}\\
&+c_1^2H_{26}\frac{\partial\psi_j^{(2)}}{\partial x}\Big]+\frac{\partial^2\varphi_i}{\partial x\partial y}\Big[-2c_1F_{26}\frac{\partial\psi_j^{(2)}}{\partial y}-2c_1F_{66}\frac{\partial\psi_j^{(2)}}{\partial x}+2c_1^2H_{26}\frac{\partial\psi_j^{(2)}}{\partial y}+2c_1^2H_{66}\frac{\partial\psi_j^{(2)}}{\partial x}\Big]\Big\}dxdy
\end{aligned}
$$

$$K_{ij}^{41} = \int_{\Omega^e} \left\{ \frac{\partial \psi_i^{(2)}}{\partial x} \left[(B_{11} - c_1 E_{11}) \frac{\partial \psi_j^{(1)}}{\partial x} + (B_{16} - c_1 E_{16}) \frac{\partial \psi_j^{(1)}}{\partial y} \right] + \frac{\partial \psi_i^{(2)}}{\partial y} \left[(B_{16} - c_1 E_{16}) \frac{\partial \psi_j^{(1)}}{\partial x} + (B_{66} - c_1 E_{66}) \frac{\partial \psi_j^{(1)}}{\partial y} \right] \right\} dxdy$$

$$K_{ij}^{42} = \int_{\Omega^e} \left\{ \frac{\partial \psi_i^{(2)}}{\partial x} \left[(B_{12} - c_1 E_{12}) \frac{\partial \psi_j^{(1)}}{\partial y} + (B_{16} - c_1 E_{16}) \frac{\partial \psi_j^{(1)}}{\partial x} \right] + \frac{\partial \psi_i^{(1)}}{\partial y} \left[(B_{26} - c_1 E_{26}) \frac{\partial \psi_j^{(1)}}{\partial y} + (B_{66} - c_1 E_{66}) \frac{\partial \psi_j^{(1)}}{\partial x} \right] \right\} dxdy$$

$$K_{ij}^{43} = \int_{\Omega^e} \left\{ \frac{\partial \psi_i^{(2)}}{\partial x} \left[\frac{1}{2} (B_{11} - c_1 E_{11}) \frac{\partial w}{\partial x} \frac{\partial \varphi_j}{\partial x} + \frac{1}{2} (B_{12} - c_1 E_{12}) \frac{\partial w}{\partial y} \frac{\partial \varphi_j}{\partial y} + \frac{1}{2} (B_{16} - c_1 E_{16}) \left(\frac{\partial w}{\partial x} \frac{\partial \varphi_j}{\partial y} + \frac{\partial w}{\partial y} \frac{\partial \varphi_j}{\partial x} \right) + c_1 (c_1 H_{11} - F_{11}) \frac{\partial^2 \varphi_j}{\partial x^2} + c_1 (c_1 H_{12} - F_{12}) \frac{\partial^2 \varphi_j}{\partial y^2} + 2c_1 (c_1 H_{16} - F_{16}) \frac{\partial^2 \varphi_j}{\partial x \partial y} \right] + \frac{\partial \psi_i^{(2)}}{\partial y} \left[\frac{1}{2} (B_{16} - c_1 E_{16}) \frac{\partial w}{\partial x} \frac{\partial \varphi_j}{\partial x} + \frac{1}{2} (B_{26} - c_1 E_{26}) \frac{\partial w}{\partial y} \frac{\partial \varphi_j}{\partial y} + \frac{1}{2} (B_{66} - c_1 E_{66}) \left(\frac{\partial w}{\partial x} \frac{\partial \varphi_j}{\partial y} + \frac{\partial w}{\partial y} \frac{\partial \varphi_j}{\partial x} \right) + c_1 (c_1 H_{16} - F_{16}) \frac{\partial^2 \varphi_j}{\partial x^2} + c_1 (c_1 H_{26} - F_{26}) \frac{\partial^2 \varphi_j}{\partial y^2} + 2c_1 (H_{66} - c_1 F_{66}) \frac{\partial^2 \varphi_j}{\partial x \partial y} \right] + \psi_i^{(2)} \left[(A_{55} - 2c_2 D_{55} + c_2^2 F_{55}) \frac{\partial \varphi_j}{\partial x} + (A_{45} - 2c_2 D_{45} + c_2^2 F_{45}) \frac{\partial \varphi_j}{\partial y} \right] \right\} dxdy$$

$$K_{ij}^{44} = \int_{\Omega^e} \left\{ \frac{\partial \psi_i^{(2)}}{\partial x} \left[(D_{11} - 2c_1 F_{11} + c_1^2 H_{11}) \frac{\partial \psi_j^{(2)}}{\partial x} + (D_{16} - 2c_1 F_{16} + c_1^2 H_{16}) \frac{\partial \psi_j^{(2)}}{\partial y} \right] + \frac{\partial \psi_i^{(2)}}{\partial y} \left[(D_{16} - 2c_1 F_{16} + c_1^2 H_{16}) \frac{\partial \psi_j^{(2)}}{\partial x} + (D_{66} - 2c_1 F_{66} + c_1^2 H_{66}) \frac{\partial \psi_j^{(2)}}{\partial y} \right] + \psi_i^{(2)} \left[(A_{55} - 2c_2 D_{55} + c_2^2 F_{55}) \psi_j^{(2)} \right] \right\} dxdy$$

$$K_{ij}^{45} = \int_{\Omega^e} \left\{ \frac{\partial \psi_i^{(2)}}{\partial x} \left[(D_{12} - 2c_1 F_{12} + c_1^2 H_{12}) \frac{\partial \psi_j^{(2)}}{\partial y} + (D_{16} - 2c_1 F_{16} + c_1^2 H_{16}) \frac{\partial \psi_j^{(2)}}{\partial x} \right] + \frac{\partial \psi_i^{(2)}}{\partial y} \left[(D_{26} - 2c_1 F_{26} + c_1^2 H_{26}) \frac{\partial \psi_j^{(2)}}{\partial y} + (D_{66} - 2c_1 F_{66} + c_1^2 H_{66}) \frac{\partial \psi_j^{(2)}}{\partial x} \right] + \psi_i^{(2)} \left[(A_{45} - 2c_2 D_{45} + c_2^2 F_{45}) \psi_j^{(2)} \right] \right\} dxdy$$

$$K_{ij}^{51} = \int_{\Omega^e} \left\{ \frac{\partial \psi_i^{(2)}}{\partial x} \left[(B_{16} - c_1 E_{16}) \frac{\partial \psi_j^{(1)}}{\partial x} + (B_{66} - c_1 E_{66}) \frac{\partial \psi_j^{(1)}}{\partial y} \right] + \frac{\partial \psi_i^{(1)}}{\partial y} \left[(B_{12} - c_1 E_{12}) \frac{\partial \psi_j^{(1)}}{\partial x} + (B_{26} - c_1 E_{26}) \frac{\partial \psi_j^{(1)}}{\partial y} \right] \right\} dxdy$$

$$K_{ij}^{52} = \int_{\Omega^e} \left\{ \frac{\partial \psi_i^{(2)}}{\partial x} \left[(B_{26} - c_1 E_{26}) \frac{\partial \psi_j^{(1)}}{\partial y} + (B_{66} - c_1 E_{66}) \frac{\partial \psi_j^{(1)}}{\partial x} \right] + \frac{\partial \psi_i^{(1)}}{\partial y} \left[(B_{22} - c_1 E_{22}) \frac{\partial \psi_j^{(1)}}{\partial y} + (B_{26} - c_1 E_{26}) \frac{\partial \psi_j^{(1)}}{\partial x} \right] \right\} dxdy$$

$$K_{ij}^{53} = \int_{\Omega^e} \left\{ \frac{\partial \psi_i^{(2)}}{\partial x} \left[\frac{1}{2} (B_{16} - c_1 E_{16}) \frac{\partial w}{\partial x} \frac{\partial \varphi_j}{\partial x} + \frac{1}{2} (B_{26} - c_1 E_{26}) \frac{\partial w}{\partial y} \frac{\partial \varphi_j}{\partial y} + \frac{1}{2} (B_{66} - c_1 E_{66}) \left(\frac{\partial w}{\partial x} \frac{\partial \varphi_j}{\partial y} + \frac{\partial w}{\partial y} \frac{\partial \varphi_j}{\partial x} \right) + c_1 (c_1 H_{16} - F_{16}) \frac{\partial^2 \varphi_j}{\partial x^2} + c_1 (c_1 H_{26} - F_{26}) \frac{\partial^2 \varphi_j}{\partial y^2} + 2c_1 (c_1 H_{66} - F_{66}) \frac{\partial^2 \varphi_j}{\partial x \partial y} \right] + \frac{\partial \psi_i^{(2)}}{\partial y} \left[\frac{1}{2} (B_{12} - c_1 E_{12}) \frac{\partial w}{\partial x} \frac{\partial \varphi_j}{\partial x} + \frac{1}{2} (B_{22} - c_1 E_{22}) \frac{\partial w}{\partial y} \frac{\partial \varphi_j}{\partial y} \right.$$

$$+\frac{1}{2}(B_{26}-c_1E_{26})\left(\frac{\partial w}{\partial x}\frac{\partial\varphi_j}{\partial y}+\frac{\partial w}{\partial y}\frac{\partial\varphi_j}{\partial x}\right)+c_1(c_1H_{12}-F_{12})\frac{\partial^2\varphi_j}{\partial x^2}+c_1(c_1H_{22}-F_{22})\frac{\partial^2\varphi_j}{\partial y^2}$$
$$+2c_1(H_{26}-c_1F_{26})\frac{\partial^2\varphi_j}{\partial x\partial y}\Big]+\psi_i^{(2)}\Big[(A_{45}-2c_2D_{45}+c_2^2F_{45})\frac{\partial\varphi_j}{\partial x}$$
$$+(A_{44}-2c_2D_{44}+c_2^2F_{44})\frac{\partial\varphi_j}{\partial y}\Big]\Big\}dxdy$$

$$K_{ij}^{54}=\int_{\Omega^e}\Big\{\frac{\partial\psi_i^{(2)}}{\partial x}\Big[(D_{16}-2c_1F_{16}+c_1^2H_{16})\frac{\partial\psi_j^{(2)}}{\partial x}+(D_{66}-2c_1F_{66}+c_1^2H_{66})\frac{\partial\psi_j^{(2)}}{\partial y}\Big]$$
$$+\frac{\partial\psi_i^{(2)}}{\partial y}\Big[(D_{12}-2c_1F_{12}+c_1^2H_{12})\frac{\partial\psi_j^{(2)}}{\partial x}+(D_{26}-2c_1F_{26}+c_1^2H_{26})\frac{\partial\psi_j^{(2)}}{\partial y}\Big]$$
$$+\psi_i^{(2)}\Big[(A_{45}-2c_2D_{45}+c_2^2F_{45})\psi_j^{(2)}\Big]\Big\}dxdy$$

$$K_{ij}^{55}=\int_{\Omega^e}\Big\{\frac{\partial\psi_i^{(2)}}{\partial x}\Big[(D_{26}-2c_1F_{26}+c_1^2H_{26})\frac{\partial\psi_j^{(2)}}{\partial y}+(D_{66}-2c_1F_{66}+c_1^2H_{66})\frac{\partial\psi_j^{(2)}}{\partial x}\Big]$$
$$+\frac{\partial\psi_i^{(2)}}{\partial y}\Big[(D_{22}-2c_1F_{22}+c_1^2H_{22})\frac{\partial\psi_j^{(2)}}{\partial y}+(D_{26}-2c_1F_{26}+c_1^2H_{26})\frac{\partial\psi_j^{(2)}}{\partial x}\Big]$$
$$+\psi_i^{(2)}\Big[(A_{44}-2c_2D_{44}+c_2^2F_{44})\psi_j^{(2)}\Big]\Big\}dxdy$$

$$F_i^1=\oint_{\Gamma^e}(N_{xx}\hat{n}_x+N_{xy}\hat{n}_y)\psi_i^{(1)}ds,\quad F_i^2=\oint_{\Gamma^e}(N_{xy}\hat{n}_x+N_{yy}\hat{n}_y)\psi_i^{(1)}ds$$
$$0=\int_{\Omega^e}q(1-\mu\nabla^2)\varphi_i dxdy+\oint_{\Gamma^e}\Big\{(\bar{Q}_x\hat{n}_x+\bar{Q}_y\hat{n}_y)+(N_{xx}w_{0,x}+N_{xy}w_{0,y})\hat{n}_x$$
$$+(N_{xy}w_{0,x}-N_{yy}w_{0,y})\hat{n}_y+c_1\Big[P_{xx,x}\hat{n}_x+P_{yy,y}\hat{n}_y+(P_{xy,x}\hat{n}_y+P_{xy,y}\hat{n}_x)\Big]$$
$$-c_1\Big[P_{xx}\hat{n}_x+P_{yy}\hat{n}_y+(P_{xy}\hat{n}_y+P_{xy}\hat{n}_x)\Big]\Big\}ds$$
$$F_i^4=\oint_{\Gamma^e}(M_{xx}\hat{n}_x+M_{xy}\hat{n}_y)\psi_i^{(2)}ds,\quad F_i^5=\oint_{\Gamma^e}(M_{xy}\hat{n}_x+M_{yy}\hat{n}_y)\psi_i^{(2)}ds$$

Appendix C

Tangent stiffness matrix term's

$$T_{ij}^{11}=K_{ij}^{11}+\sum_{\gamma=1}^{5}\sum_{k=1}^{n}\frac{\partial K_{ik}^{1\gamma}}{\partial u_j}\Delta_k^\gamma=K_{ij}^{11},\quad T_{ij}^{12}=K_{ij}^{12}+\sum_{\gamma=1}^{5}\sum_{k=1}^{n}\frac{\partial K_{ik}^{1\gamma}}{\partial v_j}\Delta_k^\gamma=K_{ij}^{12}$$
$$T_{ij}^{13}=K_{ij}^{13}+\sum_{\gamma=1}^{5}\sum_{k=1}^{n}\frac{\partial K_{ik}^{1\gamma}}{\partial w_j}\Delta_k^\gamma=K_{ij}^{13}+\sum_{k=1}^{n}\frac{\partial K_{ik}^{13}}{\partial w_j}w_k$$
$$=K_{ij}^{13}+\int_{\Omega^e}\Big\{\frac{\partial\psi_i^{(1)}}{\partial x}\Big[\frac{1}{2}A_{11}\frac{\partial w}{\partial x}\frac{\partial\varphi_j}{\partial x}+\frac{1}{2}A_{12}\frac{\partial w}{\partial y}\frac{\partial\varphi_j}{\partial y}+\frac{1}{2}A_{16}\Big(\frac{\partial w}{\partial x}\frac{\partial\varphi_j}{\partial y}+\frac{\partial w}{\partial y}\frac{\partial\varphi_j}{\partial x}\Big)$$
$$+\frac{\partial\psi_i^{(1)}}{\partial y}\Big[\frac{1}{2}A_{16}\frac{\partial w}{\partial x}\frac{\partial\varphi_j}{\partial x}+\frac{1}{2}A_{26}\frac{\partial w}{\partial y}\frac{\partial\varphi_j}{\partial y}+\frac{1}{2}A_{66}\Big(\frac{\partial w}{\partial x}\frac{\partial\varphi_j}{\partial y}+\frac{\partial w}{\partial y}\frac{\partial\varphi_j}{\partial x}\Big)\Big]\Big\}dxdy=T_{ji}^{31}$$
$$T_{ij}^{14}=K_{ij}^{14}+\sum_{\gamma=1}^{5}\sum_{k=1}^{n}\frac{\partial K_{ik}^{1\gamma}}{\partial X_j}\Delta_k^\gamma=K_{ij}^{14},\quad T_{ij}^{15}=K_{ij}^{15}+\sum_{\gamma=1}^{5}\sum_{k=1}^{n}\frac{\partial K_{ik}^{1\gamma}}{\partial Y_j}\Delta_k^\gamma=K_{ij}^{15}$$
$$T_{ij}^{21}=K_{ij}^{21}+\sum_{\gamma=1}^{5}\sum_{k=1}^{n}\frac{\partial K_{ik}^{2\gamma}}{\partial u_j}\Delta_k^\gamma=K_{ij}^{21},\quad T_{ij}^{22}=K_{ij}^{22}+\sum_{\gamma=1}^{5}\sum_{k=1}^{n}\frac{\partial K_{ik}^{2\gamma}}{\partial v_j}\Delta_k^\gamma=K_{ij}^{22}$$

$$
\begin{aligned}
T_{ij}^{23} &= K_{ij}^{23} + \sum_{\gamma=1}^{5}\sum_{k=1}^{n}\frac{\partial K_{ik}^{2\gamma}}{\partial w_j}\Delta_k^{\gamma} = K_{ij}^{23} + \sum_{k=1}^{n}\frac{\partial K_{ik}^{23}}{\partial w_j}w_k \\
&= K_{ij}^{23} + \int_{\Omega^e}\Bigg\{\frac{\partial \psi_i^{(1)}}{\partial x}\Big[\frac{1}{2}A_{16}\frac{\partial w}{\partial x}\frac{\partial \varphi_j}{\partial x} + \frac{1}{2}A_{26}\frac{\partial w}{\partial y}\frac{\partial \varphi_j}{\partial y} + \frac{1}{2}A_{66}\Big(\frac{\partial w}{\partial x}\frac{\partial \varphi_j}{\partial y} + \frac{\partial w}{\partial y}\frac{\partial \varphi_j}{\partial x}\Big) \\
&\quad + \frac{\partial \psi_i^{(1)}}{\partial y}\Big[\frac{1}{2}A_{12}\frac{\partial w}{\partial x}\frac{\partial \varphi_j}{\partial x} + \frac{1}{2}A_{22}\frac{\partial w}{\partial y}\frac{\partial \varphi_j}{\partial y} + \frac{1}{2}A_{26}\Big(\frac{\partial w}{\partial x}\frac{\partial \varphi_j}{\partial y} + \frac{\partial w}{\partial y}\frac{\partial \varphi_j}{\partial x}\Big)\Big]\Bigg\}dxdy = T_{ji}^{32} \\
T_{ij}^{24} &= K_{ij}^{24} + \sum_{\gamma=1}^{5}\sum_{k=1}^{n}\frac{\partial K_{ik}^{2\gamma}}{\partial X_j}\Delta_k^{\gamma} = K_{ij}^{24}, \quad T_{ij}^{25} = K_{ij}^{25} + \sum_{\gamma=1}^{5}\sum_{k=1}^{n}\frac{\partial K_{ik}^{2\gamma}}{\partial Y_j}\Delta_k^{\gamma} = K_{ij}^{25} \\
T_{ij}^{31} &= K_{ij}^{31} + \sum_{\gamma=1}^{5}\sum_{k=1}^{n}\frac{\partial K_{ik}^{3\gamma}}{\partial u_j}\Delta_k^{\gamma} = K_{ij}^{31}, \quad T_{ij}^{32} = K_{ij}^{32} + \sum_{\gamma=1}^{5}\sum_{k=1}^{n}\frac{\partial K_{ik}^{3\gamma}}{\partial v_j}\Delta_k^{\gamma} = K_{ij}^{32} \\
T_{ij}^{33} &= K_{ij}^{33} + \sum_{\gamma=1}^{5}\sum_{k=1}^{n}\frac{\partial K_{ik}^{3\gamma}}{\partial w_j}\Delta_k^{\gamma} \\
&= K_{ij}^{33} + \sum_{k=1}^{n}\Big(\frac{\partial K_{ik}^{31}}{\partial w_j}u_k + \frac{\partial K_{ik}^{32}}{\partial w_j}v_k + \frac{\partial K_{ik}^{33}}{\partial w_j}w_k + \frac{\partial K_{ik}^{34}}{\partial w_j}X_k + \frac{\partial K_{ik}^{35}}{\partial w_j}Y_k\Big) - \frac{\partial F_i^{3T}}{\partial w_j} \\
&= K_{ij}^{33} + \int_{\Omega^e}\Big[\frac{\partial \varphi_i}{\partial x}\Big(A_{11}\frac{\partial u}{\partial x}\frac{\partial \psi_j^{(1)}}{\partial x} + A_{16}\frac{\partial u}{\partial x}\frac{\partial \psi_j^{(1)}}{\partial y} + A_{16}\frac{\partial u}{\partial y}\frac{\partial \psi_j^{(1)}}{\partial x} + A_{66}\frac{\partial u}{\partial y}\frac{\partial \psi_j^{(1)}}{\partial y}\Big) \\
&\quad + \frac{\partial \varphi_i}{\partial y}\Big(A_{16}\frac{\partial u}{\partial x}\frac{\partial \psi_j^{(1)}}{\partial x} + A_{66}\frac{\partial u}{\partial x}\frac{\partial \psi_j^{(1)}}{\partial y} + A_{12}\frac{\partial u}{\partial y}\frac{\partial \psi_j^{(1)}}{\partial x} + A_{26}\frac{\partial u}{\partial y}\frac{\partial \psi_j^{(1)}}{\partial y}\Big)\Big]dxdy \\
&\quad + \int_{\Omega^e}\Big[\frac{\partial \varphi_i}{\partial x}\Big(A_{12}\frac{\partial v}{\partial x}\frac{\partial \psi_j^{(1)}}{\partial y} + A_{16}\frac{\partial v}{\partial x}\frac{\partial \psi_j^{(1)}}{\partial x} + A_{26}\frac{\partial v}{\partial y}\frac{\partial \psi_j^{(1)}}{\partial y} + A_{66}\frac{\partial v}{\partial y}\frac{\partial \psi_j^{(1)}}{\partial x}\Big) \\
&\quad + \frac{\partial \varphi_i}{\partial y}\Big(A_{26}\frac{\partial v}{\partial x}\frac{\partial \psi_j^{(1)}}{\partial y} + A_{66}\frac{\partial v}{\partial x}\frac{\partial \psi_j^{(1)}}{\partial x} + A_{22}\frac{\partial v}{\partial y}\frac{\partial \psi_j^{(1)}}{\partial y} + A_{26}\frac{\partial v}{\partial y}\frac{\partial \psi_j^{(1)}}{\partial x}\Big)\Big]dxdy \\
&\quad + \int_{\Omega^e}\Big[\Big(A_{11}\Big(\frac{\partial w}{\partial x}\Big)^2 + A_{12}\Big(\frac{\partial w}{\partial y}\Big)^2 + 2A_{16}\frac{\partial w}{\partial x}\frac{\partial w}{\partial y}\Big)\frac{\partial \varphi_i}{\partial x}\frac{\partial \varphi_j}{\partial x} \\
&\quad + \Big(A_{16}\Big(\frac{\partial w}{\partial x}\Big)^2 + A_{26}\Big(\frac{\partial w}{\partial y}\Big)^2 + 2A_{66}\frac{\partial w}{\partial x}\frac{\partial w}{\partial y}\Big)\Big(\frac{\partial \varphi_i}{\partial x}\frac{\partial \varphi_j}{\partial y} + \frac{\partial \varphi_i}{\partial y}\frac{\partial \varphi_j}{\partial x}\Big) \\
&\quad + \Big(A_{12}\Big(\frac{\partial w}{\partial x}\Big)^2 + A_{22}\Big(\frac{\partial w}{\partial y}\Big)^2 + 2A_{26}\frac{\partial w}{\partial x}\frac{\partial w}{\partial y}\Big)\frac{\partial \varphi_i}{\partial y}\frac{\partial \varphi_j}{\partial y} \\
&\quad + \frac{\partial \varphi_i}{\partial x}\Big(-c_1E_{11}\frac{\partial w}{\partial x}\frac{\partial^2 \varphi_j}{\partial x^2} - c_1E_{12}\frac{\partial w}{\partial x}\frac{\partial^2 \varphi_j}{\partial y^2} - 2E_{16}\frac{\partial w}{\partial x}\frac{\partial \varphi_j}{\partial x\partial y} - c_1E_{16}\frac{\partial w}{\partial y}\frac{\partial^2 \varphi_j}{\partial x^2} - c_1E_{26}\frac{\partial w}{\partial y}\frac{\partial^2 \varphi_j}{\partial y^2} - 2E_{66}\frac{\partial w}{\partial y}\frac{\partial \varphi_j}{\partial x\partial y}\Big) \\
&\quad + \frac{\partial \varphi_i}{\partial y}\Big(-c_1E_{16}\frac{\partial w}{\partial x}\frac{\partial^2 \varphi_j}{\partial x^2} - c_1E_{26}\frac{\partial w}{\partial x}\frac{\partial^2 \varphi_j}{\partial y^2} - 2E_{66}\frac{\partial w}{\partial x}\frac{\partial \varphi_j}{\partial x\partial y} - c_1E_{12}\frac{\partial w}{\partial y}\frac{\partial^2 \varphi_j}{\partial x^2} - c_1E_{22}\frac{\partial w}{\partial y}\frac{\partial^2 \varphi_j}{\partial y^2} - 2E_{26}\frac{\partial w}{\partial y}\frac{\partial \varphi_j}{\partial x\partial y}\Big) \\
&\quad + \frac{\partial^2 \varphi_i}{\partial x^2}\Big(-\frac{1}{2}c_1E_{11}\frac{\partial w}{\partial x}\frac{\partial \varphi_j}{\partial x} - \frac{1}{2}c_1E_{12}\frac{\partial w}{\partial y}\frac{\partial \varphi_j}{\partial y} + \frac{1}{2}E_{16}\Big(\frac{\partial w}{\partial x}\frac{\partial \varphi_j}{\partial y} + \frac{\partial w}{\partial y}\frac{\partial \varphi_j}{\partial x}\Big)\Big) \\
&\quad + \frac{\partial^2 \varphi_i}{\partial y^2}\Big(-\frac{1}{2}c_1E_{12}\frac{\partial w}{\partial x}\frac{\partial \varphi_j}{\partial x} - \frac{1}{2}c_1E_{22}\frac{\partial w}{\partial y}\frac{\partial \varphi_j}{\partial y} + \frac{1}{2}E_{26}\Big(\frac{\partial w}{\partial x}\frac{\partial \varphi_j}{\partial y} + \frac{\partial w}{\partial y}\frac{\partial \varphi_j}{\partial x}\Big)\Big) \\
&\quad + \frac{\partial^2 \varphi_i}{\partial x\partial y}\Big(-c_1E_{16}\frac{\partial w}{\partial x}\frac{\partial \varphi_j}{\partial x} - c_1E_{26}\frac{\partial w}{\partial x}\frac{\partial \varphi_j}{\partial x} - c_1E_{66}\Big(\frac{\partial w}{\partial x}\frac{\partial \varphi_j}{\partial y} + \frac{\partial w}{\partial y}\frac{\partial \varphi_j}{\partial x}\Big)\Big)\Big]dxdy \\
&\quad + \int_{\Omega^e}\Bigg\{\frac{\partial \varphi_i}{\partial x}\Big[(B_{16} - c_1E_{16})\frac{\partial \psi_j^{(2)}}{\partial x}\frac{\partial \phi_x}{\partial y} + (B_{66} - c_1E_{66})\frac{\partial \psi_j^{(2)}}{\partial y}\frac{\partial \phi_x}{\partial y} \\
&\quad + (B_{11} - c_1E_{11})\frac{\partial \psi_j^{(2)}}{\partial x}\frac{\partial \phi_x}{\partial x} + (B_{16} - c_1E_{16})\frac{\partial \psi_j^{(2)}}{\partial y}\frac{\partial \phi_x}{\partial x}\Big] \\
&\quad + \frac{\partial \varphi_i}{\partial y}\Big[(B_{66} - c_1E_{66})\frac{\partial \psi_j^{(2)}}{\partial y}\frac{\partial \phi_x}{\partial x} + (B_{16} - c_1E_{16})\frac{\partial \psi_j^{(2)}}{\partial x}\frac{\partial \phi_x}{\partial x} \\
&\quad + (B_{12} - c_1E_{12})\frac{\partial \psi_j^{(2)}}{\partial x}\frac{\partial \phi_x}{\partial y} + (B_{26} - c_1E_{26})\frac{\partial \psi_j^{(2)}}{\partial y}\frac{\partial \phi_x}{\partial y}\Big]\Bigg\}dxdy
\end{aligned}
$$

$$+\int_{\Omega^e}\left\{\frac{\partial\varphi_i}{\partial x}\left[(B_{12}-c_1E_{12})\frac{\partial\psi_j^{(2)}}{\partial y}\frac{\partial\phi_y}{\partial x}+(B_{16}-c_1E_{16})\frac{\partial\psi_j^{(2)}}{\partial x}\frac{\partial\phi_y}{\partial x}\right.\right.$$
$$\left.+(B_{26}-c_1E_{26})\frac{\partial\psi_j^{(2)}}{\partial y}\frac{\partial\phi_y}{\partial y}+(B_{66}-c_1E_{66})\frac{\partial\psi_j^{(2)}}{\partial x}\frac{\partial\phi_y}{\partial y}\right]$$
$$+\frac{\partial\varphi_i}{\partial y}\left[(B_{26}-c_1E_{26})\frac{\partial\psi_j^{(2)}}{\partial y}\frac{\partial\phi_y}{\partial x}+(B_{66}-c_1E_{66})\frac{\partial\psi_j^{(2)}}{\partial x}\frac{\partial\phi_y}{\partial x}\right.$$
$$\left.\left.+(B_{22}-c_1E_{22})\frac{\partial\psi_j^{(2)}}{\partial y}\frac{\partial\phi_y}{\partial y}+(B_{26}-c_1E_{26})\frac{\partial\psi_j^{(2)}}{\partial x}\frac{\partial\phi_y}{\partial y}\right]\right\}dxdy$$

$$T_{ij}^{34}=K_{ij}^{34}+\sum_{\gamma=1}^{5}\sum_{k=1}^{n}\frac{\partial K_{ik}^{3\gamma}}{\partial X_j}\Delta_k^{\gamma}=K_{ij}^{34},\quad T_{ij}^{35}=K_{ij}^{35}+\sum_{\gamma=1}^{5}\sum_{k=1}^{n}\frac{\partial K_{ik}^{3\gamma}}{\partial Y_j}\Delta_k^{\gamma}=K_{ij}^{35}$$

$$T_{ij}^{41}=K_{ij}^{41}+\sum_{\gamma=1}^{5}\sum_{k=1}^{n}\frac{\partial K_{ik}^{4\gamma}}{\partial u_j}\Delta_k^{\gamma}=K_{ij}^{41},\quad T_{ij}^{42}=K_{ij}^{42}+\sum_{\gamma=1}^{5}\sum_{k=1}^{n}\frac{\partial K_{ik}^{4\gamma}}{\partial v_j}\Delta_k^{\gamma}=K_{ij}^{42}$$

$$T_{ij}^{43}=K_{ij}^{43}+\sum_{\gamma=1}^{5}\sum_{k=1}^{n}\frac{\partial K_{ik}^{4\gamma}}{\partial w_j}\Delta_k^{\gamma}=K_{ij}^{43}+\sum_{k=1}^{n}\frac{\partial K_{ik}^{43}}{\partial w_j}w_k$$
$$=K_{ij}^{43}+\int_{\Omega^e}\left\{\frac{\partial\psi_i^{(2)}}{\partial x}\left[\frac{1}{2}(B_{11}-c_1E_{11})\frac{\partial w}{\partial x}\frac{\partial\varphi_j}{\partial x}+\frac{1}{2}(B_{12}-c_1E_{12})\frac{\partial w}{\partial y}\frac{\partial\varphi_j}{\partial y}\right.\right.$$
$$\left.+\frac{1}{2}(B_{16}-c_1E_{16})\left(\frac{\partial w}{\partial x}\frac{\partial\varphi_j}{\partial y}+\frac{\partial w}{\partial y}\frac{\partial\varphi_j}{\partial x}\right)\right]+\frac{\partial\psi_i^{(2)}}{\partial y}\left[\frac{1}{2}(B_{16}-c_1E_{16})\frac{\partial w}{\partial x}\frac{\partial\varphi_j}{\partial x}\right.$$
$$\left.\left.+\frac{1}{2}(B_{26}-c_1E_{26})\frac{\partial w}{\partial y}\frac{\partial\varphi_j}{\partial y}+\frac{1}{2}(B_{66}-c_1E_{66})\left(\frac{\partial w}{\partial x}\frac{\partial\varphi_j}{\partial y}+\frac{\partial w}{\partial y}\frac{\partial\varphi_j}{\partial x}\right)\right]\right\}dxdy=T_{ji}^{34}$$

$$T_{ij}^{44}=K_{ij}^{44}+\sum_{\gamma=1}^{5}\sum_{k=1}^{n}\frac{\partial K_{ik}^{4\gamma}}{\partial X_j}\Delta_k^{\gamma}=K_{ij}^{44},\quad T_{ij}^{45}=K_{ij}^{45}+\sum_{\gamma=1}^{5}\sum_{k=1}^{n}\frac{\partial K_{ik}^{4\gamma}}{\partial Y_j}\Delta_k^{\gamma}=K_{ij}^{45}$$

$$T_{ij}^{51}=K_{ij}^{51}+\sum_{\gamma=1}^{5}\sum_{k=1}^{n}\frac{\partial K_{ik}^{5\gamma}}{\partial u_j}\Delta_k^{\gamma}=K_{ij}^{51},\quad T_{ij}^{52}=K_{ij}^{52}+\sum_{\gamma=1}^{5}\sum_{k=1}^{n}\frac{\partial K_{ik}^{5\gamma}}{\partial v_j}\Delta_k^{\gamma}=K_{ij}^{52}$$

$$T_{ij}^{53}=K_{ij}^{53}+\sum_{\gamma=1}^{5}\sum_{k=1}^{n}\frac{\partial K_{ik}^{5\gamma}}{\partial w_j}\Delta_k^{\gamma}=K_{ij}^{53}+\sum_{k=1}^{n}\frac{\partial K_{ik}^{53}}{\partial w_j}w_k$$
$$=K_{ij}^{53}+\int_{\Omega^e}\left\{\frac{\partial\psi_i^{(2)}}{\partial x}\left[\frac{1}{2}(B_{16}-c_1E_{16})\frac{\partial w}{\partial x}\frac{\partial\varphi_j}{\partial x}+\frac{1}{2}(B_{26}-c_1E_{26})\frac{\partial w}{\partial y}\frac{\partial\varphi_j}{\partial y}\right.\right.$$
$$\left.+\frac{1}{2}(B_{66}-c_1E_{66})\left(\frac{\partial w}{\partial x}\frac{\partial\varphi_j}{\partial y}+\frac{\partial w}{\partial y}\frac{\partial\varphi_j}{\partial x}\right)\right]+\frac{\partial\psi_i^{(2)}}{\partial y}\left[\frac{1}{2}(B_{12}-c_1E_{12})\frac{\partial w}{\partial x}\frac{\partial\varphi_j}{\partial x}\right.$$
$$\left.\left.+\frac{1}{2}(B_{22}-c_1E_{22})\frac{\partial w}{\partial y}\frac{\partial\varphi_j}{\partial y}+\frac{1}{2}(B_{26}-c_1E_{26})\left(\frac{\partial w}{\partial x}\frac{\partial\varphi_j}{\partial y}+\frac{\partial w}{\partial y}\frac{\partial\varphi_j}{\partial x}\right)\right]\right\}dxdy=T_{ji}^{35}$$

$$T_{ij}^{54}=K_{ij}^{54}+\sum_{\gamma=1}^{5}\sum_{k=1}^{n}\frac{\partial K_{ik}^{5\gamma}}{\partial X_j}\Delta_k^{\gamma}=K_{ij}^{54},\quad T_{ij}^{55}=K_{ij}^{55}+\sum_{\gamma=1}^{5}\sum_{k=1}^{n}\frac{\partial K_{ik}^{5\gamma}}{\partial Y_j}\Delta_k^{\gamma}=K_{ij}^{55}$$

Supplementary material

Supplementary material associated with this article can be found, in the online version, at 10.1016/j.ijengsci.2017.12.006.

References

Aghababaei, R., & Reddy, J. N. (2009). Nonlocal third-order shear deformation plate theory with application to bending and vibration of plates. *Journal of Sound and Vibration, 326*, 277–289.

Aliaga, J. W., & Reddy, J. N. (2004). Nonlinear thermoelastic analysis of functionally graded plates using the third-order shear deformation theory. *International Journal of Computational Engineering Science, 5*(4), 753–779.

Aller, E. M., Drar, C., Schilz, J., & Kaysser, W. A. (2003). Functionally graded materials for sensor and energy applications. *Materials Science and Engineering A, 362*(12), 1739.

Arash, B., & Wang, Q. (2012). A review on the application of nonlocal elastic models in modeling of carbon nanotubes and graphenes. *Computational Materials Science, 51*(1), 303–313.
Bažant, Z. P., & Milan, J. (2002). Nonlocal integral formulations of plasticity and damage. *American Society of Civil Engineers, 128*, 11–19.
Benveniste. , Y. (1987). A new approach to the application of Mori–Tanaka's theory in composite materials. *Mechanics of Materials, 6*, 147–157.
Birman, V., & Byrd, L. W. (2007). Modelling and analysis of functionally graded materials and structures. *Applied Mechanics Reviews, 60*, 195–216.
Challamel, N., & Wang, C. M. (2008). The small length scale effect for a non-local cantilever beam: A paradox solved. *Nanotechnology, 19*(34), 345703. 7
Edelen, D. G. B., & Laws, N. (1971). On the thermodynamics of systems with nonlocality. *Archives of Rational Mechanics and Analysis, 43*, 24–35.
Elishakoff, I., & Gentilini, C. (2005). Three-dimensional flexure of rectangular plates made of functionally graded materials. *Journal of Applied Mechanics, ASME, 72*, 788791.
Eringen, A. C. (1972). Nonlocal polar elastic continua. *International Journal of Engineering Science, 10*, 1–16.
Eringen, A. C. (1983). On differential equations of nonlocal elasticity and solutions of screw dislocation and surface waves. *Journal of Applied Physics, 54*, 47034710.
Eringen, A. C. (1998). *Microcontinuum filed theories – I: Foundations and solids*. Springer-Verlag.
Eringen, A. C. (2002). *Nonlocal continuum field theories*. New York: Springer.
Eringen, A. C., & Edelen, D. G. B. (1972). On nonlocal elasticity. *International Journal of Engineering Science, 10*, 233248.
Fernández-Sáez, J., Zaeraa, R., Loyaa, J. A., & Reddy, J. N. (2016). Bending of Euler–Bernoulli beams using Eringen's integral formulation: A paradox resolved. *International Journal of Engineering Science, 99*, 107–116.
Ferreira, A. J. M., Batra, R. C., Rouque, C. M. C., Qian, L. F., & Martins, P. A. L. S. (2005). Static analysis of functionally graded plates using third-order shear deformation theory and a Meshless method. *Composite Structures, 69*, 449–457.
Qian, L. F., Batra, R. C., & Chen, L. M. (2004). Static and dynamic deformations of thick functionally graded elastic plates by using higher-order shear and normal deformable plate theory and Meshless local Petrov–Galerkin method. *Composites Part B: Engineering, 35*, 685–697.
Golmakani, M. E., & Kadkhodayan, M. (2011). Nonlinear bending analysis of annular FGM plates using higher-order shear deformation plate theories. *Composite Structures, 93*, 973982.
Hashin, Z., & Shtrikman, S. (1962). On some variational principles in anisotropic and non homogeneous elasticity. *Journal of Mechanics and Physics of Solids, 10*(4), 335342.
Ghayesh, M. H., Farokhi, H., Gholipour, A., & Tavallaeinejad, M. (2017). Nonlinear bending and forced vibrations of axially functionally graded tapered microbeams. *International Journal of Engineering Science, 120*, 51–62.
Hosseini-Hashemi, S., Taher, H. R. D., Akhavan, H., & Omidi, M. (2010). Free vibration of functionally graded rectangular plates using first-order shear deformation plate theory. *Applied Mathematical Modelling, 34*, 12761291.
Jandaghian, A. A., & Rahmani, O. (2016). Vibration analysis of functionally graded piezoelectric nanoscale plates by nonlocal elasticity theory: An analytical solution. *Superlattices and Microstructures, 100*, 57–75.
Lee, S. J., & Reddy, J. N. (2004). Nonlinear deflection control of laminated plates using third-order shear deformation theory. *International Journal of Mechanics and Materials in Design, 1*, 3361.
John, P., George, R. B., & Richard, P. M. (2003). Application of nonlocal continuum models to nano technology. *International Journal of Engineering Science, 128*, 305–312.
Kashtalyan. , M. (2004). Three-dimensional elasticity solution for bending of functionally graded rectangular plates. *European Journal of Mechanics A/Solids, 23*, 853864.
Kim, J., & Reddy, J. N. (2015). A general third-order theory of functionally graded plates with modified couple stress effect and the von Kármán nonlinearity, theory and finite element analysis. *Acta Mechanica, 226*(9), 9732998.
Klusemann, B., & Svendsen, B. (2010). Homogenization methods for multi-phase elastic composites: Comparison and benchmarks. *Technische Mechanik, 30*(4), 374–386.
Koizumi, M. (1993). Concept of FGM. *Ceramic Transactions, 34*, 310.
Koizumi, M. (1997). FGM activities in Japan. *Composites Part B, 28*(12), 14.
Kröner, E. (1967). Elasticity theory of materials with long range cohesive forces. *International Journal of solids and structures, 3*, 731–742.
Krumhansl, J. E. (1968). Some considerations on the relations between solid state physics and generalized continuum mechanics. In *Proceedings of the 1968 international union of theoretical and applied mechanics, IUTAM symposia* (pp. 298–311).
Kunin, I. A. (1984). On foundations of the theory of elastic media with micro structure, International Journal of Engineering Science 22, 969–978.
Matsunaga, H. (2009). Stress analysis of functionally graded plates subjected to thermal and mechanical loadings. *Composite Structures, 87*, 344357.
Mori, T., & Tanaka, K. (1973). Average stress in matrix and average elastic energy of materials with misfitting inclusions. *Acta Metallurgica, 21*, 571–574.
Mousavi, S. M., Paavola, J., & Reddy, J. N. (2015). Variational approach to dynamic analysis of third-order shear deformable plates within gradient elasticity. *Meccanica, 50*(6), 1537–1550.
Nejad, M. Z., & Hadi, A. (2016). Eringen's non-local elasticity theory for bending analysis of bi-directional functionally graded Euler–Bernoulli nano-beams. *International Journal of Engineering Science, 106*, 1–9.
Reddy, J. N. (1984). A simple higher-order theory for laminated composite plates. *Journal of Applied Mechanics, 51*, 745752.
Reddy, J. N., & Wang, C. M. (1998). Deflection relationships between classical and third-order plate theories. *Acta Mechanica, 130*(34), 199208.
Pompe, W., Worch, H., Epple, M., Friess, W., Gelinsky, M., Greil, P., et al. (2003). Functionally graded materials for biomedical applications. *Materials Science and Engineering A, 362*(12), 4060.
Praveen, G. N., & Reddy, J. N. (1998). Nonlinear transient thermoelastic analysis of functionally graded ceramic-metal plates. *Journal of Solids and Structures, 35*(33), 44574476.
Raghu, P., Rajagopal, A., & Reddy, J. N. (2018). Nonlocal nonlinear finite element analysis of composite plates. *Composite Structures, 185*, 38–50.
Rahaeifard, M., Kahrobaiyan, M. H., Ahmadian, M. T., & Firoozbakhsh, K. (2013). Strain gradient formulation of functionally graded nonlinear beams. *International Journal of Engineering Science, 65*, 49–63.
Rahmani, O., & Pedram, O. (2014). Analysis and modeling the size effect on vibration of functionally graded nanobeams based on nonlocal Timoshenko beam theory. *International Journal of Engineering Science, 77*, 55–70.
Reddy, J. N. (2000). Analysis of functionally graded plates. *International Journal of Numerical Methods in Engineering, 47*(13), 663–684.
Reddy, J. N. (2004). Mechanics of laminated composite plates and shells. *Theory and analysis* ((2nd ed.)). Boca Raton, FL: CRC Press.
Reddy, J. N. (2007a). Nonlocal theories for bending, buckling and vibration of beams. *International Journal of Engineering Science, 45*, 288307.
Reddy, J. N. (2007b). *Theory of elastic plates and shells* ((2nd ed.)). CRC Press.
Reddy, J. N. (2010). Nonlocal nonlinear formulations for bending of classical and shear deformation theories of beams and plates. *International Journal of Engineering Science, 48*(11), 15071518.
Reddy, J. N. (2015). *An introduction to nonlinear finite element analysis*. UK: Oxford University Press, Oxford.
Reddy, J. N., & Cheng, Z.-Q. (2001). Three dimensional thermomechanical deformations of functionally graded rectangular plates. *European Journal of Mechanics A/Solids, 20*, 841–855.
Reddy, J. N., & Chin, C. D. (1998). Thermo mechanical analysis of functionally graded cylinders and plates. *Journal of Thermal Stresses, 21*, 593–626.
Reddy, J. N., El-Borgi, S., & Romanoff, J. (2014). Non-linear analysis of functionally graded microbeams using Eringen's non-local differential model. *International Journal of Non-Linear Mechanics, 67*, 308–318.
Reddy, J. N., & Kim, J. (2012). A nonlinear modified couple stress-based third-order theory of functionally graded plates. *Composite Structures, 94*, 11281143.
Hill, R. (1952). The elastic behavior of a crystalline aggregate. *Proceedings of Physical Society A, 65*, 34954.

Romano, G., Barretta, R., Diaco, M., & de Sciarra, F. M. (2017). Constitutive boundary conditions and paradoxes in nonlocal elastic nanobeams. *International Journal of Mechanical Sciences, 121*, 151–156.
Roque, C. M. C., Ferreira, A. J. M., & Reddy, J. N. (2011). Analysis of Timoshenko nanobeams with a nonlocal formulation and Meshless method. *International Journal of Engineering Science, 49*, 976–984.
Salehipour, H., Shahidi, A. R., & Nahvi, H. (2015). Modified nonlocal elasticity theory for functionally graded materials. *International Journal of Engineering Science, 90*, 44–57.
Schulz, U., Peters, M., Bach, F. W., & Tegeder, G. (2003). Graded coatings for thermal, wear and corrosion barriers. *Materials Science and Engineering A, 362*(12), 6180.
Shen, H.-S., & Wang, Z.-X. (2012). Assessment of Voigt and Mori–Tanaka models for vibration analysis of functionally graded plates. *Composite Structures, 94*, 2197–2208.
Simsek, M., & Yurtcu, H. H. (2013). Analytical solutions for bending and buckling of functionally graded nano beams based on the nonlocal Timoshenko beam theory. *Composite Structures, 97*, 378386.
Singha, M. K., Prakash, T., & Ganapathi, M. (2011). Finite element analysis of functionally graded plates under transverse load. *Finite Elements in Analysis and Design, 47*, 453–460.
Vel, S. S., & Batra, R. C. (2002). Exact solution for thermoelastic deformations of functionally graded thick rectangular plates. *AIAA Journal, 40*(7), 14211433.
Talha, M., & Singh, B. N. (2010). Static response and free vibration analysis of FGM plates using higher order shear deformation theory. *Applied Mathematical modeling, 34*(12), 3991–4011.
Thai, H.-T. (2012). A nonlocal beam theory for bending, buckling, and vibration of nanobeams. *International Journal of Engineering Science, 52*, 56–64.
Watari, F., Yokoyama, A., Saso, F., & Kawasaki, T. (1997). Fabrication and properties of functionally graded dental implant. *Composites Part B, 28*(12), 5–11.
Willis, J. R. (1977). Bounds and self-consistent estimates for the overall properties of anisotropic composites. *Journal of Mechanics and Physics of Solids, 25*(3), 185202.
Zhou, Z.-G., Han, J.-C., & Du, S.-Y. (1999). Investigation of a griffith crack subject to anti-plane shear by using the nonlocal theory. *International Journal of solids and structures, 36*, 3891–3901.
Zuiker, J. R. (1995). Functionally graded materials choice of micro mechanics model and limitations in property variation. *Composites Engineering, 5*(7), 807–819.